HELSINKI INSTITUTE OF PHYSICS INTERNAL REPORT SERIES

HIP-2019-02

Cosmology with Higgs inflation

Eemeli Tomberg

Helsinki Institute of Physics and
Department of Physics, Faculty of Science
University of Helsinki
Finland

ACADEMIC DISSERTATION

To be presented, with the permission of the Faculty of Science of the University of Helsinki, for public criticism in the auditorium A110 at Chemicum, A. I. Virtasen aukio 1, Helsinki, on the 18th of October 2019 at 12 o'clock.

Helsinki 2019

ISBN 978-951-51-1281-1 (print)
ISBN 978-951-51-1282-8 (pdf)
ISSN 1455-0563
http://ethesis.helsinki.fi
Unigrafia
Helsinki 2019

Much human ingenuity has gone into finding the ultimate Before.
The current state of knowledge can be summarized thus:
In the beginning there was nothing, which exploded.

— Terry Pratchett, *Lords and Ladies*

E. Tomberg: Cosmology with Higgs inflation,
University of Helsinki, 2019, 52 pages,
Helsinki Institute of Physics, Internal Report Series, HIP-2019-02,
ISBN 978-951-51-1281-1,
ISSN 1455-0563.

Abstract

Cosmic inflation is a hypothetical period in the early universe, where the expansion of space accelerated. Inflation explains many properties of the observed universe, but its cause is not known. Higgs inflation is a model where inflation is caused by the Higgs field of the Standard Model of particle physics, coupled non-minimally to gravity. In this thesis, we study various aspects of cosmology with Higgs inflation.

Inflation leaves marks on the cosmic microwave background radiation, and these marks can be used to distinguish inflationary models from each other. We study hilltop Higgs inflation, a model where quantum corrections produce a local maximum into the Higgs potential, and show that there the predicted tensor-to-scalar ratio $r \lesssim 1.2 \times 10^{-3}$. This is smaller than the prediction of tree-level Higgs inflation by a factor of four or more and can be probed by next-generation microwave telescopes.

We also study reheating, the process where the universe transitions from inflation to radiation domination with a thermal bath of relativistic Standard Model particles. We show that in Higgs inflation, reheating is particularly efficient in the Palatini formulation of general relativity, because there Higgs bosons are produced violently by a tachyonic instability. The duration of reheating affects, for example, the predicted spectral index of the primordial perturbations.

Finally, we discuss the production of primordial black holes in Higgs inflation. We show that large quantities of such black holes can be produced, but in order to satisfy observational constraints on large scales, they must be so small that they would have evaporated by now by Hawking radiation. However, if the evaporating black holes left behind Planck mass relics, these could constitute part or all of the dark matter, the dominant, unknown matter component of the universe.

Together, these studies show that even though the ingredients that go into Higgs inflation are simple, they lead to a rich phenomenology and offer valuable insights into inflation, gravitational degrees of freedom and the origin of dark matter.

Acknowledgements

I would like to thank my supervisors Syksy Räsänen and Kari Enqvist and collaborators Vera-Maria Enckell and Javier Rubio for their guidance, support, and contribution into the work that eventually became my thesis. Syksy Räsänen deserves special thanks for guiding my path as a young physicist, all the way from supervising my bachelor's and master's theses back in 2013–2016 to mentoring me during my graduate studies and providing feedback on this manuscript. Thanks also to the pre-examiners of this thesis, Isabella Masina and Daniel Figueroa, for their useful comments.

I thank the Vilho, Yrjö and Kalle Väisälä Foundation of the Finnish Academy of Science and Letters for providing funding for my graduate studies in 2017–2019, and the Doctoral Programme in Particle Physics and Universe Sciences and the Otto A. Malm Foundation for travel grants that have helped me promote my work and integrate into the research community.

I also thank the staff and other PhD students in the physics department of the University of Helsinki, especially my roommates from our notorious office A313. They have provided invaluable peer support and insights into life inside and outside of academia and helped me weigh my own future plans.

Finally, I wish to express my gratitude to all other people in my life who have made these years memorable and enjoyable. Special thanks go to my family and all the awesome folk at Alter Ego, the roleplaying association of the University of Helsinki. May the echoes of our games ring ever on.

List of included papers

This thesis is based on the following publications [1–3]:

I Higgs inflation at the hilltop
V.-M. Enckell, K. Enqvist, S. Räsänen and E. Tomberg
JCAP **1806**, 005 (2018). [arXiv:1802.09299]

II Preheating in Palatini Higgs inflation
J. Rubio and E. Tomberg
JCAP **1904**, 021 (2019). [arXiv:1902.10148]

III Planck scale black hole dark matter from Higgs inflation
S. Räsänen and E. Tomberg
JCAP **1901**, 038 (2019). [arXiv:1810.12608]

In all of the papers the authors are listed alphabetically according to particle physics convention.

The author's contribution

In paper **I**, the author carried out all analytical calculations and part of the numerical analysis. In paper **II**, the author completed most of the analytical calculations and carried out the numerical analysis. In paper **III**, the author performed essentially all analytical and numerical calculations. In all papers, the author did most of the writing for the sections on theoretical analysis and numerical results and participated in writing the other sections.

Contents

Chapter 1

Introduction

Cosmology is a science that studies the structure and evolution of the universe. In recent decades, thanks to advances in observational methods, we have been able to probe the past of the cosmos to unprecedented accuracy. Today, our best understanding of the early history of the universe is the following.

At early times, the universe went through a period of accelerated expansion of space known as cosmic inflation. During inflation, all energy was stored in a scalar field called the inflaton. The universe was almost homogeneous and isotropic, except for small perturbations seeded by quantum mechanical effects. When inflation ended, the process of reheating transferred the energy into a hot plasma of relativistic particles of the Standard Model of particle physics (SM), and the radiation-dominated era began.

As the universe continued to expand, its temperature decreased. Eventually, matter went through the electroweak phase transition, where the Standard Model Higgs field acquired its current vacuum expectation value, giving the other SM particles their masses as measured today. Later, quarks were bound into hadrons in the QCD phase transition. When the universe was a few minutes old, these hadrons formed light atomic nuclei, mainly hydrogen and helium, in the Big Bang nucleosynthesis.

Throughout these early times, the universe was opaque to light: positively and negatively charged particles filled the space, and any emitted photon was quickly reabsorbed. This changed in recombination, where charged particles formed electrically neutral atoms. Afterwards, light rays could pass through space freely, and even today we can detect this early light as the cosmic microwave background (CMB) radiation, an afterglow that carries information on the early conditions of the universe. The primordial perturbations generated during inflation can be seen as anisotropies in this radiation, and they also seeded the formation of structure when they started to grow later in the history of the universe.

By the time of recombination, radiation domination had ended and cold matter was the prevailing energy component of the universe. However, most of it did not consist of atoms, but of dark matter, a yet unknown form of energy that interacts with ordinary matter mainly through gravitation. The presence of dark matter is seen in the CMB anisotropies and in the

formation and dynamics of galaxies and galaxy clusters. The exact nature of dark matter and cosmic inflation are some of the outstanding mysteries of modern cosmology, together with other conundrums such as baryogenesis, the process which produced more matter than antimatter in the early universe, and the observed late-time acceleration of the expansion of space.

In this thesis, we study Higgs inflation, a particular solution to the problem of cosmic inflation. In Higgs inflation, the Higgs field of the Standard Model of particle physics drives inflation. When the Higgs field is coupled non-minimally to gravity, the model matches cosmological observations well, and as models of inflation go, it is elegant: no new degrees of freedom beyond the Standard Model need to be introduced to make inflation happen. Higgs inflation also provides an intriguing link between the physics on the largest, cosmological scales, and the small-scale particle physics studied by collider experiments.

The original scientific contributions of this thesis consist of three research papers. In the first paper [1], we study hilltop Higgs inflation, a special case of Higgs inflation where the Higgs potential has a local maximum. The topic of the second paper [2] is reheating in Higgs inflation, in the Palatini formulation of general relativity. The third paper [3] deals with the formation of primordial black holes in Higgs inflation; such black holes are a potential dark matter candidate.

The thesis is structured as follows. Chapter 2 is an introduction to cosmic inflation, with an emphasis on the connection between cosmological observations and the inflaton potential. In chapter 3, we study the Higgs field and its quantum-corrected potential, both with and without the non-minimal coupling. Chapter 4 combines these ingredients into Higgs inflation, and we compare hilltop Higgs inflation to other possible scenarios. In chapter 5, we discuss reheating in Higgs inflation and the differences that arise there between the metric and Palatini formulations of general relativity. Formation of primordial black holes in Higgs inflation, and their possible role as dark matter, is the topic of chapter 6. Finally, the concluding remarks are presented in chapter 7.

1.1 Notation

Throughout the thesis, we use the $(-,+,+,+)$ convention for the metric tensor. We also use natural units where the speed of light c, the reduced Planck constant $\hbar$, and the mass scale of gravitation M are set to one. Here M is the coupling multiplying the curvature scalar R in the Einstein–Hilbert action:

$$S_{\rm EH} = \frac{1}{2}\int d^4x\sqrt{-g}M^2R\,, \tag{1.1}$$

where g is the determinant of the metric $g_{\mu\nu}$. The value of M is usually equal to the (physical, measured) reduced Planck mass $M_{\rm Pl} \approx 2.4\times10^{18}$ GeV, but they differ slightly in the presence of the non-minimal gravitational coupling ξ introduced in section 3.2. Then $M_{\rm Pl}^2 = M^2 + \xi v^2$, where v is the Higgs vacuum expectation value, and $\xi v^2 \ll M^2$.

Chapter 2

Cosmic inflation

Cosmic inflation is a hypothetical time period in the very early universe before the events of the hot radiation-dominated era, where the expansion of space was accelerating. It explains the spatial flatness and large-scale homogeneity of the observed universe, features that are otherwise unexplained by the Big Bang model. Moreover, inflation explains the origin of the perturbations from which cosmic structures such as galaxies and galaxy clusters emerge. In inflationary models, these perturbations were originally quantum vacuum fluctuations that were stretched and amplified to cosmic scales during inflation. Nowadays we see imprints of these fluctuations in the CMB radiation and the large-scale structure of the universe and test models of inflation by comparing their predictions to these observations.

In this chapter, we discuss cosmic inflation on a general level. We explain how a scalar field can drive inflation, how perturbations of this field are calculated, and how these calculations can be compared to CMB measurements.

2.1 Friedmann–Robertson–Walker model

In modern cosmology, the universe is described by general relativity, a theory which combines space and time and matter using the language of differential geometry. Equations of motion for the spacetime and matter are obtained by extremizing the action [4]

$$S = \frac{1}{2}\int d^4x\sqrt{-g}R + S_{\text{mat}}\,, \tag{2.1}$$

where g is the determinant of the spacetime metric $g_{\mu\nu}$, R is the curvature scalar, and S_{mat} is the action for the matter fields.

On large scales, the observed universe is close to homogeneous and isotropic. To model this we restrict our attention to homogeneous and isotropic solutions of general relativity, which are described by the Friedmann–Robertson–Walker (FRW) metric [4]:

$$ds^2 = -dt^2 + a^2(t)\left[\frac{dr^2}{1-kr^2} + r^2\Big(d\theta^2 + \sin^2\theta d\phi^2\Big)\right], \tag{2.2}$$

where t is the cosmic time, r, θ and ϕ are the radial and angular coordinates of space, $a(t)$ is the scalar factor that describes the expansion of space, and k is a curvature constant. Plugging the metric (2.2) into action (2.1) and demanding that variations of S with respect to the metric vanish, we get the Friedmann equations:

$$H^2 = \frac{\rho}{3} - \frac{k}{a^2}\,, \qquad \frac{\ddot{a}}{a} = -\frac{1}{6}(\rho + 3p)\,, \tag{2.3}$$

where $H \equiv \frac{\dot{a}}{a}$ is the Hubble parameter, and a dot denotes a derivative with respect to t. Due to the symmetries, matter is described by an ideal fluid whose energy density ρ and pressure p are defined in the stress-energy tensor

$$T_{\mu\nu} \equiv -\frac{2}{\sqrt{-g}}\frac{\delta S_{\text{mat}}}{\delta g^{\mu\nu}} = (\rho + p)u_\mu u_\nu + p g_{\mu\nu}\,, \tag{2.4}$$

where $u^\mu = (1, 0, 0, 0)$ is the fluid's 4-velocity. Given an equation of state for matter, that is, an additional relationship between ρ, p and a, the time evolution of these quantities can be solved.

If the universe is filled with radiation and non-relativistic matter, it expands in a decelerating manner: $\ddot{a} < 0$. Going towards early times, a decreases and the energy density and temperature increase, until an initial singularity is reached some 14 billion years ago. However, a model with $\ddot{a} < 0$ all the way through has certain shortcomings when applied to the observed universe.

2.1.1 Need for inflation

The first shortcoming of the basic model presented above is that measurements indicate that the k-term in (2.3) is zero or vanishingly small compared to the energy density term, that is, space is very close to Euclidean. Since no value of k is preferred by the theory, this can be seen as fine-tuning. What's worse, if k is non-zero, the ratio between the energy density and curvature terms evolves as

$$\frac{d}{dt}\left|\frac{k}{a^2\rho}\right| = -\frac{6|k|}{a^4\rho^2}\dot{a}\ddot{a}\,, \tag{2.5}$$

where we assumed $\rho > 0$. In an expanding universe, $\dot{a} > 0$, and in a universe dominated by radiation and non-relativistic matter, $\ddot{a} < 0$, so the contribution of the curvature term grows. Even a small deviation from zero at early times could grow to a large value today, and to avoid this, the early value of this term needs to be fine-tuned very close to zero. This is the flatness problem.

Additionally, it is not clear why the universe would be homogeneous and isotropic from the very beginning. Uniform temperature of the observed CMB radiation tells us that homogeneity and isotropy apply already at an early time, and if the universe was always dominated by radiation and non-relativistic matter, then there was no time for signals to propagate from one patch of the CMB sky to another far-away patch between the Big Bang and recombination [5]. The cosmological particle horizon blocks the two patches from reaching a uniform temperature, apart from fine-tuned initial conditions. This is the horizon problem.

Both of these problems can be alleviated by postulating an era with $\ddot{a} > 0$ in the very early universe, called cosmic inflation [6–11]. During such an era, the ratio in (2.5) automatically decreases to a small value, and inflation also changes the expansion history so that far-away patches of the CMB sky are brought into causal contact with each other.

However, non-relativistic matter and radiation can't cause inflation. Instead, we need something more exotic, such as a uniform scalar field.

2.2 Scalar field inflation

For a canonical scalar field $\phi(x)$, the action (2.1) becomes [4]

$$S_\phi = \int d^4x\sqrt{-g}\Big[\frac{1}{2}R - \frac{1}{2}g^{\mu\nu}\partial_\mu\phi\partial_\nu\phi - V(\phi)\Big]\,, \tag{2.6}$$

where V is the potential function of the field. In the homogeneous and isotropic case where $\phi(x) = \phi(t)$, and with $k = 0$, the Friedmann equations take the form

$$H^2 = \frac{1}{3}\Big[\frac{1}{2}\dot{\phi}^2 + V(\phi)\Big]\,, \qquad \frac{\ddot{a}}{a} = -\frac{1}{3}\Big[\dot{\phi}^2 - V(\phi)\Big]\,, \tag{2.7}$$

together with the scalar field equation of motion, which is not independent but can be derived from these:

$$\ddot{\phi} + 3H\dot{\phi} + V'(\phi) = 0\,. \tag{2.8}$$

Using (2.7), we see that inflation happens when

$$V > \dot{\phi}^2 \qquad \Longleftrightarrow \qquad \epsilon_H \equiv \frac{\dot{\phi}^2}{2H^2} < 1\,, \tag{2.9}$$

that is, when the field velocity is small compared to the potential height. A scalar field that drives inflation in this manner is called the inflaton. A particularly simple and attractive special case is *slow-roll inflation* (SR), which we will discuss next.

2.2.1 Slow-roll inflation

In slow-roll inflation, in addition to (2.9), we also have [5]

$$|\ddot{\phi}| \ll 3H|\dot{\phi}| \qquad \Longleftrightarrow \qquad |\eta_H| \ll 1\,, \quad \eta_H \equiv -\frac{\ddot{\phi}}{H\dot{\phi}}\,, \tag{2.10}$$

in other words, the 'friction term' $3H\dot{\phi}$ in the field equation (2.8) dominates over the acceleration term $\ddot{\phi}$. The equations of motion become

$$3H\dot{\phi} \approx -V'\,, \qquad 3H^2 \approx V\,. \tag{2.11}$$

These are first order in time derivatives, and thus easier to solve than the full equations (2.7), (2.8).

We call ϵ_H and η_H the slow-roll parameters. They quantify the goodness of the slow-roll approximation at any given moment. When they are small, ϕ is in slow-roll, and we can use (2.11) to write them in terms of the potential and its derivatives:

$$\begin{aligned} \epsilon_H &\approx \epsilon_V \,, & \eta_H &\approx \eta_V - \epsilon_V \,, \\ \epsilon_V &\equiv \frac{1}{2}\left(\frac{V'}{V}\right)^2 \,, & \eta_V &\equiv \frac{V''}{V} \,. \end{aligned} \tag{2.12}$$

A given potential V can support slow-roll only if these parameters are small in some region. Even then, smallness of ϵ_V and η_V is not a sufficient condition for slow-roll inflation: one also needs suitable initial conditions for the field velocity and Hubble parameter. However, for a potential with a long region with ϵ_V, $\eta_V < 1$, slow-roll is an attractor solution of the full equations of motion, that is, the inflaton ends up on the slow-roll trajectory from a broad range of initial conditions [5]. This is one of the big selling points of slow-roll inflation. Rate of change of ϵ_V and η_V can be quantified by defining higher-order slow-roll parameters [12]:

$$\zeta_V \equiv \frac{V'}{V}\frac{V'''}{V} \,, \qquad \varpi_V \equiv \left(\frac{V'}{V}\right)^2 \frac{V''''}{V} \,, \qquad \ldots \tag{2.13}$$

To achieve a long period of slow-roll inflation, these parameters must also be small in the slow-roll region. Length of inflation is measured in e-folds N; in one e-fold, the scale factor a grows by a factor of Euler's number e. When the inflaton field ϕ rolls from value ϕ_1 to ϕ_2, the number of e-folds of inflation in slow-roll is, to leading SR order,

$$N \approx \int_{\phi_2}^{\phi_1} \frac{d\phi}{\sqrt{2\epsilon_V}} \,. \tag{2.14}$$

To understand slow-roll inflation, it is useful to consider an analogy from classical mechanics with a skier sliding down a hill. The skier's acceleration is given by a combination of two force terms: a gravity term which depends on the slope of the hill, and a friction term that we assume to be dominated by air resistance so that it increases with increasing velocity. If the skier starts from rest, their velocity will first increase, but so does the air resistance. Eventually, gravity and air resistance will balance each other out: the skier reaches terminal velocity, and their acceleration drops to zero. The terminal velocity depends on the slope of the hill and may change as the skier makes progress, but as long as the change in the slope is slow, the skier's velocity follows the changing terminal velocity.

In cosmic inflation, the inflaton field ϕ corresponds to the position of the skier, and the V' and $3H^2\dot{\phi}$ terms in the field equation (2.8) correspond to gravity and air resistance in the skier analogy. Slow-roll holds when the skier has reached the terminal velocity. If the slope of the hill is not too steep and does not change too rapidly—that is, if the potential slow-roll parameters are small—then this happens sooner or later; the solution is an attractor. Slow-roll inflation ends when the slope becomes too steep so that the terminal velocity grows quicker than the skier's speed.

Slow-roll models of cosmic inflation are attractive because they can easily provide a long period of inflation, but also because they predict a spectrum of scalar perturbations that matches the observations well. These perturbations are the topic of the next section.

2.3 Perturbations

In the intro of this chapter, we mentioned that inflationary models predict the shape of initial perturbations around the homogeneous and isotropic FRW background. This is done using cosmological perturbation theory, where both the field ϕ and the metric $g_{\mu\nu}$ are expanded as perturbative series around the FRW solutions; for a review, see [13]. It turns out that the resulting scalar perturbations, responsible for the inhomogeneities in the CMB temperature, can be described by one gauge-invariant quantity, the Sasaki-Mukhanov variable ν [14], whose Fourier mode functions μ_k follow to linear order the equations of motion

$$\mu_k'' + \left(k^2 - \frac{z''}{z}\right)\mu_k = 0\,, \qquad z \equiv a\frac{\dot{\phi}}{H}\,, \tag{2.15}$$

where prime denotes time derivative with respect to the conformal time, $d\eta = \frac{dt}{a(t)}$. This variable is then quantized, resulting in a free quantum field theory in a time-dependent background, where the perturbation configuration is fully determined by the mode functions μ_k. The quantized perturbations are taken to be initially in an adiabatic Bunch–Davies vacuum state [15], from which they evolve according to the equation of motion (2.15). At later times, perturbation field correlation functions give information on the statistical properties of the perturbations. At linear order, this process produces Gaussian perturbations with variance $|\mu_k|^2$.

When calculating the perturbations of the CMB, a particularly useful quantity is the comoving curvature perturbation $\mathcal{R}$. It is an inherently geometric quantity that describes the curvature of spacetime, but during inflation it is coupled to ν so that [16]

$$\mathcal{R} = \frac{\nu}{z}\,, \tag{2.16}$$

and for Gaussian perturbations, its statistics are fully described by its power spectrum,

$$\mathcal{P}_\mathcal{R}(k) \equiv \frac{k^3}{2\pi^2}\left\langle |\mathcal{R}_k|^2 \right\rangle = \frac{k^3}{2\pi^2}\frac{|\mu_k|^2}{z^2}\,. \tag{2.17}$$

Under fairly general conditions, Fourier components $\mathcal{R}_k$ freeze to constant values when the scales become super-Hubble, $k \ll aH$ [17]. During inflation, the quantity aH increases, so a mode with a fixed k starts from $k \gg aH$ (sub-Hubble) in the adiabatic vacuum state, evolves until it crosses the Hubble radius to super-Hubble scales, and freezes there. After inflation ends, aH decreases, so at some point the mode re-enters the Hubble radius and starts to evolve again. The strategy for solving the evolution of the perturbations is then as follows: during inflation, we use quantum field theory to solve for the time evolution of μ_k until it crosses the Hubble radius; then, we calculate the frozen value of $\mathcal{P}_\mathcal{R}(k)$ from (2.17) on the super-Hubble scales; and

after inflation, we use the frozen $\mathcal{P}_\mathcal{R}(k)$ as a statistical initial condition for classical metric and matter perturbations as the corresponding scales start to re-enter the Hubble radius.

In addition to the scalar perturbations, tensor perturbations h_{ij} are generated in inflation. Their mode functions ψ_k follow equations of motion similar to (2.15), but with $z = a$ [5],

$$\psi_k'' + \left(k^2 - \frac{a''}{a}\right)\psi_k = 0\,. \tag{2.18}$$

Tensor perturbations correspond to gravitational waves. They are created by similar quantum effects as the scalar perturbations, but at linear order, they propagate through space unhindered, without interactions with matter. The statistical properties of tensor perturbations are given by their power spectrum

$$\mathcal{P}_\mathcal{T}(k) \equiv \frac{k^3}{2\pi^2}\left\langle h_{ij}h^{ij}\right\rangle = \frac{8k^3}{2\pi^2}|\Psi_k|^2\,, \tag{2.19}$$

analogously to (2.17), where the factor eight comes from the number of polarization modes and their normalization. The power spectrum is usually discussed in terms of the tensor-to-scalar ratio, $r \equiv \frac{\mathcal{P}_\mathcal{T}}{\mathcal{P}_\mathcal{R}}$. In principle, primordial gravitational waves can be observed in the CMB polarization map as B-modes, but strong foreground effects make this challenging, and there is no detection to this date [18, 19].

2.3.1 CMB observables

CMB observations give information on primordial perturbations at largest scales observable on the sky, around the pivot scale $k_* = 0.05$ Mpc^{-1}. On these scales, CMB observations by the Planck satellite combined with other cosmological data sets give [18]

$$A_s \equiv \mathcal{P}_\mathcal{R}(k_*) = 2.1 \times 10^{-9} \tag{2.20}$$

for the scalar perturbation power spectrum and

$$\begin{gathered} n_s \equiv 1 + \frac{d\mathcal{P}_\mathcal{R}(k)}{d\ln k} = 0.9625 \pm 0.0048\,, \\ \alpha_s \equiv \frac{d^2\mathcal{P}_\mathcal{R}(k)}{d(\ln k)^2} = 0.002 \pm 0.010\,, \qquad \beta_s \equiv \frac{d^3\mathcal{P}_\mathcal{R}(k)}{d(\ln k)^3} = 0.010 \pm 0.013 \end{gathered} \tag{2.21}$$

for the spectral index n_s and higher derivatives of $\mathcal{P}_\mathcal{R}(k)$, where the derivatives are evaluated at $k = k_*$. Here n_s is slightly below one, and values of the higher derivatives are consistent with zero. Observations also give a bound

$$r \equiv \frac{\mathcal{P}_\mathcal{T}(k_*)}{\mathcal{P}_\mathcal{R}(k_*)} < 0.079 \tag{2.22}$$

for the tensor-to-scalar ratio.

2.3.2 Perturbations from slow-roll inflation

Mode equation (2.15) can be solved in slow-roll inflation to give the frozen super-Hubble value of $\mathcal{P}_\mathcal{R}(k)$ to a wanted order in the SR parameters. To leading order [5],

$$\mathcal{P}_\mathcal{R}(k) \approx \frac{V}{24\pi^2\epsilon_V}\,, \tag{2.23}$$

and the derivatives of $\mathcal{P}_\mathcal{R}(k)$ and the tensor-to-scalar ratio to leading slow-roll order are [20]

$$\begin{aligned} &n_s = 1 - 6\epsilon_V + 2\eta_V\,, \qquad r = 16\epsilon_V\,, \qquad \alpha_s = 16\epsilon_V\eta_V - 24\epsilon_V^2 - 2\zeta_V\,, \\ &\beta_s = -192\epsilon_V^3 + 192\epsilon_V^2\eta_V - 32\epsilon_V\eta_V^2 - 24\epsilon_V\zeta_V + 2\eta_V\zeta_V + 2\varpi_V\,, \end{aligned} \tag{2.24}$$

where everything is evaluated at the time when the corresponding scale left the Hubble radius.

In typical models of inflation, the pivot scale $k_* = 0.05\ \mathrm{Mpc}^{-1}$ left the Hubble radius roughly 50 to 60 e-folds before the end of inflation [5]. Using (2.14), one can find the corresponding field value, calculate the quantities (2.24) from the potential, and compare the model to the CMB observations. Note that in such a calculation, it is assumed that the universe is already isotropic, homogeneous and spatially flat at the Hubble exit of k_*, that is, some inflation has already taken place. Generally speaking, slow-roll models can match the observations very well, since by (2.24) they predict a n_s value that is close to one, in accordance with the observations (2.21). Current bounds on n_s, r, α_s and β_s favour slow-roll models with concave and very flat potentials [18].

2.4 What drives inflation?

Thus far, we have not specified the inflaton field or details of its potential. Over the years, there have been numerous proposals for different fields and potentials, some motivated by ideas like modified gravity, supersymmetry, or string theory, others studied for their interesting phenomenology. Models of inflation with more than one field, or a more complicated action with, for example, modified kinetic terms, have also been proposed. For reviews, see [5, 21]. Even though the constraints from the CMB have helped rule out whole classes of models, many remain consistent with observations. How can we choose the right model, or at least the most promising ones for further study?

One answer to this question is to choose models that are as minimal as possible, models that involve only a few additional ingredients when compared to the standard models of particle physics and cosmology. In this regard, perhaps the most interesting model is Higgs inflation, where no new fields need to be added to the Standard Model of particle physics, as the Higgs field of the SM is the inflaton. We will study this model in detail in chapter 3. Before that, we take a look at the basic properties of the SM Higgs field in the next chapter.

Chapter 3

The Higgs field

The Standard Model of particle physics describes the elementary particles of nature and their interactions. It includes quarks and leptons which make up the known matter, gauge bosons which mediate the interactions, and the Higgs field which gives masses to other particles. Despite its shortcomings—failure to explain phenomena like dark matter, neutrino oscillations, or gravity—the success of this model is astounding, with theoretical calculations matching various measurements to a high accuracy; for a review, see [22]. In July 2012, the European Organization for Nuclear Research, CERN, announced the discovery of the Higgs boson—a manifestation of the Higgs field—at the Large Hadron Collider, completing the experimental verification of the Standard Model.

The Higgs field is interesting not only for collider experiments but also from the point of view of cosmology. It is the only scalar field in the Standard Model, and hence it can, in principle, drive cosmic inflation, as we will see in chapter 4. In this chapter, we discuss the dynamics of the Higgs field. In particular, we calculate the quantum-corrected effective potential of the field which dictates its time evolution, both in the standard case and in the presence of a non-minimal coupling to gravity.

3.1 Standard Model Higgs sector

The Standard Model Lagrangian can be written in a compressed form as [23–25]

$$\begin{aligned}\mathscr{L}_{SM} = &-\bar{\psi}_a \not{D} \psi_a - \frac{1}{4}\,\mathrm{tr}\, F_b^{\mu\nu} F_{b\,\mu\nu} \\ &- (D_\mu \Phi)^\dagger (D^\mu \Phi) - V(\Phi) \\ &- \lambda_e^i \bar{E}_L^i \cdot \Phi\, e_R - \lambda_d^{ij} \bar{Q}_L^i \cdot \Phi\, d_R^j - \lambda_u^{ij} \epsilon^{ab} \bar{Q}_{L\,a}^i \cdot \Phi_b^\dagger\, u_R^j + h.c.\,,\end{aligned} \tag{3.1}$$

where the first row describes the fermion fields ψ_a and the $SU(3)_C \times SU(2)_L \times U(1)_Y$ gauge fields, the second row describes the Higgs doublet Φ with its kinetic and potential terms, and the third row describes the Yukawa sector, couplings between the Higgs and fermions, with fermions arranged into left-handed lepton and quark doublets E_L^i and Q_L^i and right-handed

charged leptons and up and down type quarks e_R^i, d_R^i and u_R^i. Here D is the covariant derivative which for the Higgs doublet, in particular, reads

$$D_\mu \Phi = (\partial_\mu - igA_\mu^a \tau^a - \frac{i}{2} g' B_\mu)\Phi \,, \tag{3.2}$$

where A_μ^a are the $SU(2)_L$ gauge fields, τ^a are their generator matrices, B_μ is the $U(1)_Y$ gauge field, and g and g' are the gauge couplings.

Let us explore the Higgs sector more carefully. The tree-level Higgs potential $V(\Phi)$ is

$$V(\Phi) = \mu^2 \Phi^\dagger \Phi + \lambda \Big(\Phi^\dagger \Phi \Big)^2 \,, \tag{3.3}$$

where measurements indicate $\mu^2 \approx -(89 \text{ GeV})^2$ and $\lambda \approx 0.13$ at the electroweak scale [21]. Since μ^2 is negative, the potential has minima not at zero, but at all Φ_0 which satisfy

$$|\Phi_0| = \sqrt{\frac{-\mu^2}{2\lambda}} \,, \tag{3.4}$$

see figure 3.1. This leads to spontaneous symmetry breaking: one specific value of Φ_0 is chosen out of all that satisfy condition (3.4), and the $SU(2)_L$ gauge symmetry present in the Lagrangian is broken by this choice of a physical vacuum state. However, we can use the gauge symmetry to rotate the vacuum state to a convenient form. We choose

$$\Phi_0 = \frac{1}{\sqrt{2}} \begin{pmatrix} 0 \\ h_0 \end{pmatrix} \,, \qquad h_0 = \sqrt{\frac{-\mu^2}{\lambda}} \,, \tag{3.5}$$

so that in full, Φ is

$$\Phi = \frac{1}{\sqrt{2}} \begin{pmatrix} \sigma_1 + i\sigma_2 \\ h + q + i\sigma_3 \end{pmatrix} \,, \tag{3.6}$$

where q and σ_i are real valued fluctuations around the background value h and $h = h_0$ for the electroweak vacuum. Fluctuations σ_i couple to the gauge sector as described below, and q is the Higgs boson. The Higgs potential gives interaction and mass terms for these fields: in particular, the tree-level potential for h is

$$V(h) = \frac{1}{2}\mu^2 h^2 + \frac{\lambda}{4} h^4 \,, \tag{3.7}$$

and the masses for q and σ_i are

$$m_h^2 = \frac{\partial^2 V(\Phi)}{\partial h^2}\Big|_{q=\sigma_i=0} = \mu^2 + 3\lambda h^2 \,, \qquad m_{\sigma_i}^2 = \frac{\partial^2 V(\Phi)}{\partial \sigma_i^2}\Big|_{q=\sigma_i=0} = \mu^2 + \lambda h^2 \,. \tag{3.8}$$

In the gauge sector, the gauge subgroup $SU(2)_L \times U(1)_Y$ has four generators corresponding to four gauge fields, but there is only one independent linear combination of the generators which leaves the vacuum expectation value invariant in a gauge transformation. This generator corresponds to the massless photon. The other generators correspond to the $W^\pm$ and Z bosons and give three broken symmetries with three would-be Goldstone bosons, the fields σ_i from

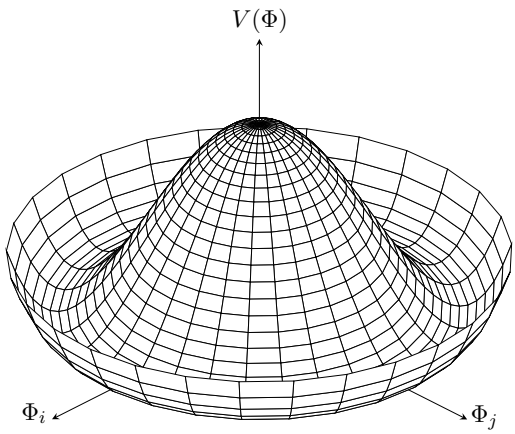

Figure 3.1: Higgs potential (3.3) in terms of two components of the complex doublet Φ. This 'Mexican hat' potential has a continuous set of minima at a non-zero value of $|\Phi|$.

(3.6). Higgs and gauge fields are coupled through the covariant derivatives (3.2) in the Higgs kinetic term in (3.1). The term quadratic in h reads

$$\mathscr{L}_{h^2} = -\frac{h^2}{8}\Big(g^2 A^a_\mu A^{a\,\mu} + g'^2 B_\mu B^\mu - 2gg' A^3_\mu B^\mu\Big)\,, \tag{3.9}$$

and in the $W^\pm$ and Z basis this gives masses to the weak gauge bosons:

$$\begin{aligned} \mathscr{L}_{h^2} &= \frac{1}{2}m_W^2\Big(W^+_\mu W^{-\mu} + W^-_\mu W^{+\mu}\Big) + \frac{1}{2}m_Z^2 Z_\mu Z^\mu\,, \\ m_W^2 &= g^2\frac{h^2}{4}\,, \quad m_Z^2 = \Big(g^2+g'^2\Big)\frac{h^2}{4}\,. \end{aligned} \tag{3.10}$$

We also get terms linear in h:

$$\begin{aligned} \mathscr{L}_h &= -\frac{h}{2}\Big(gA^3_\mu - g'B_\mu\Big)\partial^\mu\sigma_1 + g\frac{h}{2}\Big(A^2_\mu\partial^\mu\sigma_2 + A^1_\mu\partial^\mu\sigma_3\Big) \\ &= -g\frac{h}{2}\Big(W^+_\mu\partial^\mu\sigma^+ + W^-_\mu\partial^\mu\sigma^-\Big) - \sqrt{g^2+g'^2}\frac{h}{2}Z_\mu\partial^\mu\sigma_1\,, \quad \sigma^\pm \equiv -\frac{1}{\sqrt{2}}(\sigma_2 \pm i\sigma_1)\,, \end{aligned} \tag{3.11}$$

which couple $W^\pm$ and Z linearly to the would-be Goldstone bosons so that σ_i become the longitudinal degrees of freedom for the now massive gauge bosons.

The Higgs expectation value also gives mass to fermions f through the Yukawa sector in (3.1): we get mass terms of the form

$$\mathscr{L}_{m_f} = -m_f\bar{f}_L f_R\,, \qquad m_f = \frac{y_f}{\sqrt{2}}h\,. \tag{3.12}$$

Note that this designation of degrees of freedom works for any value of h, not only the one which minimizes the potential. In what follows we will work with the Higgs field expanded around a general and non-constant background value h, but the degrees of freedom for the perturbations stay the same.

3.1.1 Quantum-corrected effective potential

In Higgs inflation, the h field is taken to be the inflaton, and we would like to solve its evolution far from the electroweak vacuum (3.5). At classical level, h follows the equation of motion (2.8) with the tree-level potential (3.7). However, Φ is a quantum field, and quantum corrections to the classical solution may be important for inflation. In this section, we show how the leading corrections are calculated.

Let us start by considering a state where the Higgs doublet Φ has an arbitrary classical background value $\Phi_{\rm cl}$ with quantum perturbations expanded around this background. By 'arbitrary classical background value' we mean that $\Phi_{\rm cl}$ does not need to satisfy the vacuum condition (3.4), and that $\Phi_{\rm cl}$ is a complex-valued vector, not an operator, and the expectation value of the field operator is equal to $\Phi_{\rm cl}$. Analogously to (3.5), we rotate Φ so that always

$$\left\langle \hat{\Phi} \right\rangle = \Phi_{\rm cl} = \frac{1}{\sqrt{2}} \begin{pmatrix} 0 \\ h \end{pmatrix} , \tag{3.13}$$

where h is a real-valued function of time. Operator $\hat{\Phi}$ can then be expressed as perturbations around $\Phi_{\rm cl}$. The perturbations are taken to be in their vacuum state[1].

The effect of quantum fluctuations on the evolution of h can be taken into account by calculating the effective action [26]:

$$\Gamma(h) = -\int d^4x\sqrt{-g}\Big[V_{\rm eff}(h) + \frac{1}{2}Z(h)\nabla_\mu h\nabla^\mu h + \text{higher derivative terms}\Big] . \tag{3.14}$$

Here functions $V_{\rm eff}$, Z, and their counterparts for the higher derivative terms are obtained by summing over one-particle irreducible Feynman diagrams of all the fields that are coupled to the background field value: Higgs perturbations, fermions, and massive gauge bosons [25]. We work at next-to-leading order and consider only the leading corrections to the classical action. The value of Z can be effectively set to one by a field rescaling[2]. We neglect the terms with higher-order derivatives—they are suppressed by higher powers of the couplings and are also expected to be small when higher field derivatives are small, such as in the context of slow-roll inflation discussed in section 2.2.1. The remaining non-trivial term, $V_{\rm eff}$, is the quantum-corrected effective potential of the theory. To our next-to-leading order, it is

$$V_{\rm eff} = V_{\rm tree} + V_{1-\rm loop} , \tag{3.15}$$

where $V_{1-\rm loop}$ is the one-loop correction to the tree-level potential (3.7). For the SM Higgs, in

[1] Technically, in the effective action formalism presented here, $\Phi_{\rm cl} \equiv \langle \text{vac}_{\rm out}|\hat{\Phi}|\text{vac}_{\rm in}\rangle$, where $|\text{vac}_{\rm in}\rangle$ and $\langle \text{vac}_{\rm out}|$ are the in and out vacuums for perturbations in the distant past and future and may be different in a time-dependent background. However, we take $\Phi_{\rm cl}$ to be a good approximation of an expectation value in the adiabatic vacuum discussed in section 2.3. This seems reasonable during inflation, when the background changes slowly.

[2] This is the rescaling discussed in footnote 3.

the $\overline{MS}$ renormalization scheme and Landau gauge, the correction is [27]

$$\begin{aligned} V_{1-\text{loop}} = &\frac{m_h^4}{64\pi^2}\left(\ln\frac{m_h^2}{\mu^2}-\frac{3}{2}\right)+\frac{3m_\sigma^4}{64\pi^2}\left(\ln\frac{m_\sigma^2}{\mu^2}-\frac{3}{2}\right)\\ &+\frac{6m_W^4}{64\pi^2}\left(\ln\frac{m_W^2}{\mu^2}-\frac{5}{6}\right)+\frac{3m_Z^4}{64\pi^2}\left(\ln\frac{m_Z^2}{\mu^2}-\frac{5}{6}\right)\\ &-\frac{3m_t^4}{16\pi^2}\left(\ln\frac{m_t^2}{\mu^2}-\frac{3}{2}\right), \end{aligned} \tag{3.16}$$

where μ is the renormalization scale which appears in regularization of the loop integrals. The first two terms in (3.16) come from the Higgs and would-be Goldstone bosons with masses (3.8), the third and fourth term come from the W and Z bosons with masses (3.10), and the last term comes from the top quark with mass (see (3.12))

$$m_t = \frac{y_t h}{\sqrt{2}}, \tag{3.17}$$

where y_t is the top Yukawa coupling. We neglect other fermions: they are much lighter than the top quark, that is, their Yukawa couplings are much weaker, and their contribution to $V_{1-\text{loop}}$ is negligible.

Potential (3.16) is calculated in Minkowski spacetime, but we take it to be a good leading approximation also during inflation. To take into account leading quantum corrections in the evolution of h and the scale factor a, it is then enough to substitute $S_{\text{mat}} = \Gamma(h)$ in the action (2.1), or equivalently, to replace the tree-level potential by V_{eff} in the Friedmann equations (2.7) and the scalar field equation (2.8).

3.1.2 Running couplings

There is one important feature in our expression for V_{eff} (3.16): it depends not only on the couplings and the field value h, but also on an additional parameter μ, the renormalization scale. To relate the theory to observations, we need values not only for the couplings but also for μ. However, there is a scaling behaviour in quantum field theory which connects these parameters to each other: physical observables, such as correlation functions or solutions of the effective action, do not change in the scaling[3] [25]

$$\alpha_i \to \alpha_i + d\alpha_i\,, \quad \mu \to \mu + d\mu\,, \quad d\alpha_i = \beta_i(\alpha_j)dt\,, \quad d\mu = e^t dt\,, \tag{3.18}$$

where α_i are couplings, t is a running parameter and β_i are functions of the couplings that tell how α_i change. Solving $t = \ln\mu$ we see that the couplings 'run' as we change μ, and this renormalization group running is given by the beta functions:

$$\frac{d\alpha_i}{d\ln\mu} = \beta_i(\alpha_j)\,. \tag{3.19}$$

[3]These must be accompanied by a field strength rescaling, but in the next-to-leading order this scaling works similarly for all terms in the effective action and does not affect the equations of motion [28].

The beta functions can be solved perturbatively from the theory; in the SM, to lowest order, we have [27]

$$\begin{aligned} 16\pi^2\beta_\lambda &= -6y_t^4 + \frac{3}{8}\Big(2g^4 + \big[g^2 + g'^2\big]^2\Big) + \lambda\Big(12y_t^2 - 9g^2 - 3g'^2\Big)\,, \\ 16\pi^2\beta_{y_t} &= y_t\Big(\frac{9}{2}y_t^2 - \frac{9}{4}g^2 - \frac{17}{12}g'^2 - 8g_s^2\Big)\,, \\ 16\pi^2\beta_g &= -\frac{19}{6}g^3\,, \quad 16\pi^2\beta_{g'} = \frac{41}{6}g'^3\,, \quad 16\pi^2\beta_{g_s} = -7g_s^3\,, \end{aligned} \tag{3.20}$$

where g_s is the strong gauge coupling. Initial conditions for the running are obtained by fixing μ in the theory to a convenient value, usually close to the energy scale of experiments, and deducing values of the couplings at this μ by matching theory predictions with measurement results.

Physics stays unchanged under the renormalization group running. This is beneficial in perturbative calculations: we can run our parameters to values that make the perturbation series converge as fast as possible. In particular, in our expression for the effective potential one-loop correction (3.16), the magnitude of the logarithms may be large if μ is much smaller or larger than the particle masses which are proportional to the background field value h. In this case, the one-loop contribution becomes large, and we can't expect the higher-order terms to stay small either since they typically contain similar logarithmic terms to higher orders. Perturbativity breaks down. However, we can save the situation by choosing, say, $\mu = m_t$, while also running the couplings to the new scale. By setting μ to this h dependent value we make the logarithms small and guarantee that expression (3.16) is a good next-to-leading order approximation for V_{eff} for all field values.

3.2 Non-minimal coupling to gravity

In the next chapter, we will see that in order to make Higgs inflation compatible with observations, we need to add one more ingredient to the model. This is a non-minimal coupling between the Higgs and gravity, so that the action becomes

$$S = \int d^4x\sqrt{-g}\Big(\frac{1}{2}R + \xi R\Phi^\dagger\Phi + \mathscr{L}_{SM}\Big)\,, \tag{3.21}$$

where ξ is a new coupling parameter and $\mathscr{L}_{SM}$ is the SM Lagrangian from (3.1). The h-dependent part is

$$S_h = \int d^4x\sqrt{-g}\Big[\frac{1}{2}\big(1 + \xi h^2\big)R - \frac{1}{2}g^{\mu\nu}\partial_\mu h\partial_\nu h - V(h)\Big]\,. \tag{3.22}$$

The new ξ-term is actually a natural extension of the model: it is the only possible local scalar term of dimension four that can be added, and for a quantum field theory in curved spacetime, a counterterm of this form must in any case be added to cancel divergences in perturbation theory [15], and there is no a priori reason why the renormalized value of ξ should be zero. Indeed, we

see that the new term only becomes important when $h \gtrsim 1/\sqrt{\xi}$ in natural units. This may be true during Higgs inflation, but in today's universe, the ξ-term is insignificant unless ξ is very large. Experimentally, the tightest limits give $\xi \lesssim 10^{15}$ [29, 30]. In successful Higgs inflation, ξ typically takes values in the range $10^2 \dots 10^9$, see chapter 4. Note that large ξ-values do not spoil perturbativity since ξ is not an expansion parameter in perturbative calculations.

Action (3.22) with the non-minimal coupling term describes the model in what is called the Jordan frame. To analyse the model further, it is convenient to make a Weyl transformation to the Einstein frame, that is, to rescale the metric [31]:

$$g_{\mu\nu} = (1 + \xi h^2)^{-1} g_{E\mu\nu} \,, \tag{3.23}$$

where $g_{E\mu\nu}$ is a new metric in the new frame. This eliminates the non-minimal coupling term, but since the metric also resides in R and in the kinetic term, the kinetic sector becomes non-canonical. A canonical form is restored by defining a new scalar field χ by

$$\frac{dh}{d\chi} = \frac{1 + \xi h^2}{\sqrt{1 + \xi h^2 + 6\xi^2 h^2}} \,. \tag{3.24}$$

In terms of χ and $g_{E\mu\nu}$, the action has the simple form

$$S_\chi = \int d^4x \sqrt{-g_E} \left[\frac{1}{2} R_E - \frac{1}{2} g_E^{\mu\nu} \partial_\mu \chi \partial_\nu \chi - V_E(\chi) \right] , \tag{3.25}$$

where R_E is the curvature scalar calculated from $g_{E\mu\nu}$. The gravity part of the action is now in the standard Einstein–Hilbert form and the kinetic χ-term is canonical, so the standard analysis of, say, SR inflation from chapter 2 is applicable. All ξ-dependence is transferred into the potential V_E:

$$V_E(\chi) = \frac{V[h(\chi)]}{[1 + \xi h^2(\chi)]^2} \equiv \frac{\lambda}{4} F[h(\chi)]^4 \,, \tag{3.26}$$

where

$$F(h) = \frac{h}{\sqrt{1 + \xi h^2}} \approx \begin{cases} \chi \,, & h \ll 1/\xi \\ \frac{1}{\sqrt{\xi}} \left(1 - e^{-\sqrt{2/3}\chi} \right)^{1/2} , & h \gg 1/\sqrt{\xi} \,. \end{cases} \tag{3.27}$$

The potential is flat at $h \gg 1/\sqrt{\xi}$, see figure 3.2. We will see in chapter 4 that this property is crucial for Higgs inflation.

The problem with the potential V_E is that it is non-renormalizable, and thus it is not immediately clear how to calculate quantum corrections here like we did in the $\xi = 0$ case in section 3.1.1. This is a manifestation of the non-renormalizability of gravity, present here because we mixed the metric and Higgs degrees of freedom in the Weyl transformation. However, at large field values, when the potential becomes flat, the model can be approximated by the chiral Standard Model where the corrections can be calculated order by order. We discuss this in the next section.

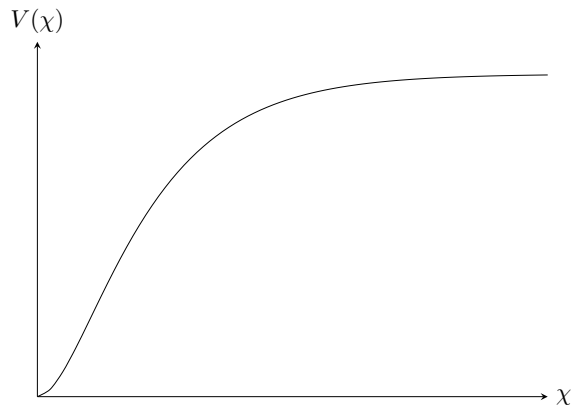

Figure 3.2: Higgs potential with a non-minimal coupling to gravity in the Einstein frame, in terms of the canonical scalar field χ, see (3.26) and (3.27). The potential has an exponentially flat plateau at large χ values.

3.2.1 Chiral Standard Model

At $h \gg 1/\sqrt{\xi}$, in the Einstein frame, the potential V_E (3.26) becomes flat and its derivatives are exponentially suppressed. Effectively, the Higgs boson decouples from the other particles, and we are left with the chiral Standard Model, an effective field theory where the Higgs degree of freedom has been integrated out of the SM [32, 33]. Even this model is not renormalizable, but the number of new counterterms needed at each loop order is finite, so perturbative calculations can be done consistently to any finite loop order. In particular, in the leading order that we are interested in, no new couplings need to be introduced.

One-loop correction to the effective potential is now [32, 34]

$$\begin{aligned} V_{E\,1-\text{loop}} = {} & \frac{6m_W^4}{64\pi^2}\left(\ln\frac{m_W^2}{\mu^2} - \frac{5}{6}\right) + \frac{3m_Z^4}{64\pi^2}\left(\ln\frac{m_Z^2}{\mu^2} - \frac{5}{6}\right) \\ & - \frac{3m_t^4}{16\pi^2}\left(\ln\frac{m_t^2}{\mu^2} - \frac{3}{2}\right), \end{aligned} \tag{3.28}$$

that is, the SM result (3.16) without the Higgs self-contributions. For masses, we use values rescaled from (3.10) and (3.17) to the Einstein frame:

$$m_W^2 = \frac{g^2F^2}{4}, \qquad m_Z^2 = \frac{(g^2+g'^2)F^2}{4}, \qquad m_t^2 = \frac{y_t^2F^2}{2}, \tag{3.29}$$

where F is the χ-dependent function from (3.27). For the renormalization scale, we choose the field-dependent value

$$\mu = \gamma F(\chi), \tag{3.30}$$

where γ is a constant of the same order as the couplings. This choice ensures that the logarithms in (3.28) remain small, as discussed in section 3.1.2. The couplings are run to this scale using the beta functions, which are slightly different for the chiral SM [32, 35]:

$$\begin{aligned}
16\pi^2\beta_\lambda &= -6y_t^4 + \frac{3}{8}\Big[2g^4 + (g'^2+g^2)^2\Big] + \lambda\Big(12y_t^2 - 6g^2 - 3g'^2\Big)\,,\\
16\pi^2\beta_{y_t} &= y_t\Big(3y_t^2 - \frac{3}{2}g^2 - \frac{17}{12}g'^2 - 8g_s^2\Big)\,,\\
16\pi^2\beta_g &= -\frac{13}{4}g^3\,, \quad 16\pi^2\beta_{g'} = \frac{27}{4}g'^3\,, \quad 16\pi^2\beta_{g_s} = -7g_s^3\,,\\
16\pi^2\beta_\xi &= -\xi\Big(3g^2 + \frac{3}{2}g'^2 - 6y_t^2\Big)\,.
\end{aligned} \tag{3.31}$$

Running of ξ and the λ-dependent term in β_λ are often ignored in Higgs inflation, since they cancel each other out in running of the ratio λ/ξ^2 present in the tree-level potential [32], and their effects are in any case sub-leading for small λ-values which are typical on large energy scales.

Using the chiral SM as an effective field theory in the high energy regime $h \gg \lambda/\sqrt{\xi}$ raises certain questions. How do we know that no new physics arises between the electroweak and inflationary scales? Such new physics could introduce new interaction terms for the Higgs and spoil the model presented here. The assumption that no such corrections arise is an assumption of simplicity: we choose to study the case where as little as possible is added to the known SM physics. One may also postulate a shift symmetry in the field on large energy scales in the Einstein frame which preserves the exponential flatness of the potential and excludes operators that would spoil this [36]; in the Jordan frame, this corresponds to scale invariance at large energies.

However, even with these assumptions, the physics on energy scales between the high energy regime and the electroweak scale is not fully known, since there is a gap between the validity of the known SM and the chiral SM approximation at $1/\xi \lesssim h \lesssim 1/\sqrt{\xi}$ [32, 36–40]. In practice, this means that the running of the couplings is not known here, but the effects of this unknown physics can be parametrized by jumps in the running couplings between the two regimes [38, 39].

3.2.2 Caveats

Apart from the unknown physics at $1/\xi \lesssim h \lesssim 1/\sqrt{\xi}$, there are also other caveats in our non-minimally coupled model, discussed extensively in the literature. One caveat is related to the choice of frames. Although physics is equivalent in the Jordan and Einstein frames at the classical level, there remains some unclarity on whether this is true in the quantized theory [36, 37, 41–46]. If not, one might end up with a different quantum-corrected Einstein frame potential depending on whether the quantum corrections are calculated before or after the transition from the Jordan frame to the Einstein frame. In particular, a natural choice for the renormalization scale (3.30) depends on the frame in which the quantum corrections are calculated [34].

Above, we chose to calculate the corrections in the Einstein frame. This corresponds to prescription I in the notation of [34]. This choice can be motivated as follows: In the Einstein frame, the problem most resembles one we know how to solve—quantum field theory in a Minkowski spacetime. The difficult-to-handle non-minimal coupling has been 'hidden away' into the potential, and the connection between the field to be quantized and the hard-to-quantize gravity is minimal. Thus we expect that the leading quantum corrections are equivalent to those computed in a Minkowski background with the Einstein frame potential, as discussed in section 3.1.1.

Another possible issue is perturbative unitarity in scattering processes, which by dimensional arguments seems to be broken in Higgs inflation near the inflationary scale [47–49]. However, a more careful analysis done in a field-dependent background shows that the typical scattering energies are always below the unitarity cut-off scale [36, 50–52]. A crucial observation is that there are many different energy scales present in the model—background energy density scale, Hubble scale, field strength, renormalization scale, typical perturbation energy scale to name just a few—that should not be confused with each other.

A third problem with Higgs inflation is the possible metastability of the electroweak vacuum in the Standard Model. According to the latest measurements of the SM parameters, if the SM (without a non-minimal coupling) is extrapolated to high energies, the Higgs effective potential may develop a secondary minimum above the electroweak scale [53, 54]; in the worst-case scenario, the Higgs self-coupling λ may run to a negative value and ruin inflation with the potential (3.26). However, the introduction of new physics at the scale $h \sim 1/\xi$ discussed in the previous section may save the situation by either interfering below the scale of the supposed secondary vacuum or by allowing λ to jump back to a positive value. At intermediary scales, thermal corrections may also raise the potential back to positive values during reheating [39]. Even if this fails, the vacuum metastability is not yet certain—latest estimates support it at the level of a few sigmas, with a large uncertainty coming from the inaccurate determination of the top quark mass [55].

3.2.3 Palatini gravity

We next discuss an alternative formulation of our non-minimally coupled model by considering the Palatini formulation of general relativity [56, 57], where the metric $g_{\mu\nu}$ and the spacetime connection $\Gamma^\alpha_{\beta\gamma}$ which defines the Ricci tensor $R_{\mu\nu}(\Gamma)$ are taken to be independent quantities. Above, we followed the usual convention where the connection is taken to be of the Levi-Civita form, that is, a function of the metric [4]:

$$\Gamma^\alpha_{\beta\gamma} = \frac{1}{2} g^{\alpha\rho}(g_{\beta\rho,\gamma} + g_{\gamma\rho,\beta} - g_{\beta\gamma,\rho})\,. \tag{3.32}$$

However, this is not a necessary assumption: instead, the metric and the connection may be treated as independent variables, so that we get independent equations of motion from the variation of S with respect to the connection. If the action is of the standard form (2.1), with a connection-dependent Einstein–Hilbert part plus a connection independent matter part, then

these new equations constrain the connection into the Levi-Civita form. However, if there is mixing between the matter and the connection, as in our non-minimally coupled Higgs model, Palatini formulation predicts different physics compared to the metric formulation [58].

In Higgs inflation, the difference manifests itself in the Weyl transformation (3.23). In Palatini formulation, $R_{\mu\nu}(\Gamma)$ is independent of $g_{\mu\nu}$, so it remains unchanged in the transformation. As a result, the needed field redefinition (3.24) is different in the Palatini case [58]:

$$\frac{dh}{d\chi} = \sqrt{1+\xi h^2}\,. \tag{3.33}$$

Again, we end up with an action of the canonical form (3.25), but the potential V_E changes. This time the relationship between h and χ can be solved and inverted analytically, so that we end up with the Einstein frame potential

$$V_E(\chi) = \frac{\lambda}{4}F^4(\chi)\,, \qquad F(\chi) \equiv \frac{1}{\sqrt{\xi}}\tanh\left(\sqrt{\xi}\chi\right). \tag{3.34}$$

This differs from the metric version (3.26)–(3.27), but has similar qualitative features, namely, it becomes exponentially flat for $h \gg 1/\sqrt{\xi}$. We again use the chiral SM to calculate the leading quantum corrections, this time with F in the mass terms given by (3.34).

Palatini formulation has the benefit that there the Einstein–Hilbert action contains only first derivatives of the quantities, while in the metric formulation second derivatives of the metric appear. For this reason, in the metric case the York–Gibbons–Hawking boundary term needs to be added to the action to produce the correct equations of motion [59, 60], but this term is not needed in the Palatini formulation. There is also no experimental reason to exclude the Palatini formulation since it predicts the same physics in today's universe where the ξ-term in action (3.21) is subdominant and the Palatini and metric predictions coincide. In the next chapter, we will see how the Palatini formulation produces different inflationary predictions compared to the metric formulation. This suggests the interesting possibility that inflationary physics may be used to probe the fundamental degrees of freedom of gravity.

Chapter 4

Higgs inflation

Since the Standard Model Higgs field is the only known fundamental scalar field, it is interesting to ask whether it could drive cosmic inflation, and if so, what are the predicted CMB observables. It turns out that the SM Higgs can indeed be the inflaton, but a non-minimal coupling to gravity is needed to match the CMB measurements. Such a model was first considered in [31] and has invoked a lot of interest since; for a review of later developments, see [61].

In this chapter, we first discuss the necessity of the non-minimal coupling ξ for successful Higgs inflation. We then go through the model's predictions for CMB observables both at tree level and with quantum corrections.

4.1 Minimally coupled Higgs as inflaton?

Let us start with the SM Higgs coupled minimally to gravity, so that its tree-level potential (3.7) is quartic at large field values. The SR parameters (2.12) read in terms of h, to lowest SR order,

$$\epsilon_V = \frac{8}{h^2}\,, \qquad \eta_V = \frac{12}{h^2}\,. \tag{4.1}$$

We see that the potential supports SR inflation at $h \gtrsim 1$. Using (2.14), h can be written in terms of the number of e-folds of inflation left N. The curvature power spectrum (2.23) becomes

$$A_s = \frac{2\lambda N^3}{3\pi^2} \qquad \Rightarrow \qquad \lambda = \frac{3\pi^2 A_s}{2N^3} \sim 10^{-13}\,, \tag{4.2}$$

where in the last approximation we used $N \approx 50$ and the observed value of A_s (2.20). The required value of λ is much smaller than the SM value $\lambda \sim 0.1$ at the electroweak scale. Moreover, the spectral index and the tensor-to-scalar ratio in the slow-roll approximation (2.24) in terms of N are

$$n_s = 1 - \frac{3}{N} \approx 0.94\,, \qquad r = \frac{16}{N} \approx 0.3\,. \tag{4.3}$$

Here n_s is multiple sigmas away from the observed value (2.21), and r is much larger than the experimental upper bound (2.22). We see that at tree level, with just a minimal coupling to

gravity, the SM Higgs can't be the inflaton. Even the quantum corrections described in section 3.1.1 cannot alleviate these problems [1, 62].

4.2 Tree-level non-minimal Higgs inflation

Introducing the non-minimal coupling ξ from section 3.2 changes things [31]. The inflationary analysis is best done in the Einstein frame. Now the Einstein frame potential (3.26) supports SR inflation on the plateau at $h \gg 1/\sqrt{\xi}$, and the leading slow-roll results are

$$n_s = 1 - \frac{2}{N}\,, \quad r = \frac{12}{N^2}\,, \quad \alpha_s = -\frac{2}{N^2}\,, \quad \beta_s = -\frac{4}{N^3}\,, \quad A_s = \frac{\lambda N^2}{72\pi^2\xi^2}\,. \tag{4.4}$$

With $N \approx 50$ and the observed value of A_s (2.20), these imply

$$n_s \approx 0.96\,, \quad r \approx 4.8\times 10^{-3}\,, \quad \alpha_s \approx -8\times 10^{-4}\,, \quad \beta_s \approx -3.2\times 10^{-5}\,, \quad \xi \approx 800\sqrt{\lambda}N\,. \tag{4.5}$$

Spectral index n_s matches the observed value in (2.21), while the values of r, α_s, and β_s are consistent with the current observational bounds and may be regarded as predictions of the model, to be confirmed or ruled out by future CMB surveys. The required value of ξ is large—$\xi \sim 10^4$ for $\lambda \sim 0.1$—but for $\lambda < 1$, it is well within the observational limits mentioned in section 3.2.

4.3 Quantum-corrected non-minimal Higgs inflation

In the previous section, we saw that adding the non-minimal coupling ξ makes the SM Higgs a viable inflaton candidate at tree level. To improve the analysis, we want to include the leading quantum corrections discussed in section 3.2.1. The unknown physics on scales $1/\xi \lesssim h \lesssim 1/\sqrt{\xi}$, parametrized by unknown jumps of the couplings, introduces uncertainty into the analysis. For a wide range of the jump values, the general shape of the exponentially flat Einstein frame potential remains unchanged, and the tree-level predictions (4.4) still apply [28]. However, for fine-tuned jumps, the quantum corrections may change the potential enough to change the predictions and expand the space of allowed values for the CMB observables. The two simplest of such cases are the critical point and hilltop scenarios, to be discussed in the next sections. Predictions for CMB observables in these cases are collected into figure 4.2.

4.3.1 Monotonic potentials with a feature

If there is a feature in the potential in the inflationary region near or below the CMB scale, this affects the CMB observables. A 'feature' here means that the first and second derivatives of the potential take unusually small values at some point; in the extreme case of a critical point, they vanish locally, see figure 4.1. Higgs inflation with such a feature has been considered in [38,39,63–69]. Such potentials are highly sensitive to the details of the quantum corrections, produce a

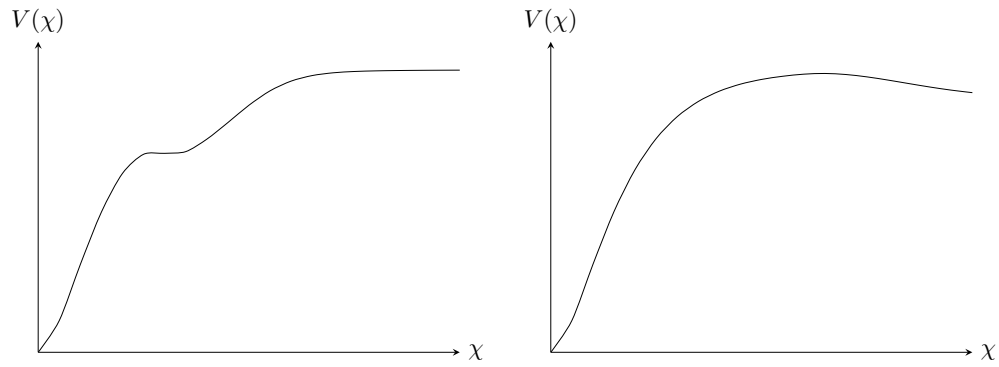

Figure 4.1: Einstein frame Higgs potentials with a feature. Left: a critical point potential where the first and second derivatives of the potential vanish locally. Right: a hilltop potential with a local maximum at the inflationary region. Compare these to the tree-level potential of figure 3.2. The features are exaggerated to make them easier to see by eye.

wide range of CMB predictions that differ from the tree-level ones, and admit smaller ξ-values. In particular, in [65], the quantum corrections were calculated according to the description of section 3.2.1, and a scan over all quantum-corrected monotonic potentials with features was performed. Despite the wide range of allowed CMB values, the authors also found combinations of CMB observables that can't be reached with such potentials, see figure 4.2.

In addition to modifying the CMB observables, a strong feature can amplify the scalar perturbations to values far exceeding the pivot scale amplitude (2.20) in other parts of the spectrum. Later in the history of the universe, these perturbations may collapse into primordial black holes and serve as dark matter. We will consider this scenario in chapter 6.

4.3.2 Hilltop inflation

In hilltop Higgs inflation, the quantum corrections generate a local maximum into the potential above the CMB scale, on the otherwise flat plateau, see figure 4.1, and the field rolls slowly from the hilltop towards the electroweak minimum. Hilltop inflation was first studied in [70]. For Higgs inflation, this scenario was first considered in [28, 67], and the details were worked out in [1], the first article of this thesis. The hilltop potential may be approximated analytically by absorbing all quantum corrections into the effective running coupling λ_{eff}, so that

$$V = \frac{\lambda_{\text{eff}}}{4} F^4 \,, \qquad V' = \frac{F^3 F'}{4} (4\lambda_{\text{eff}} + \beta_{\text{eff}}) \,, \tag{4.6}$$

where F is defined in (3.27), and β_{eff} gives the running of λ_{eff} according to (3.19), with renormalization scale given by (3.30). We see that there is a hilltop if $4\lambda_{\text{eff}} + \beta_{\text{eff}} = 0$ at some point in the renormalization group running. The CMB predictions can be calculated by expanding the potential to leading order in $\delta \equiv 1/(\xi h^2)$ and $\delta_0 \equiv 1/(\xi h_0^2)$, where index 0 refers to the position

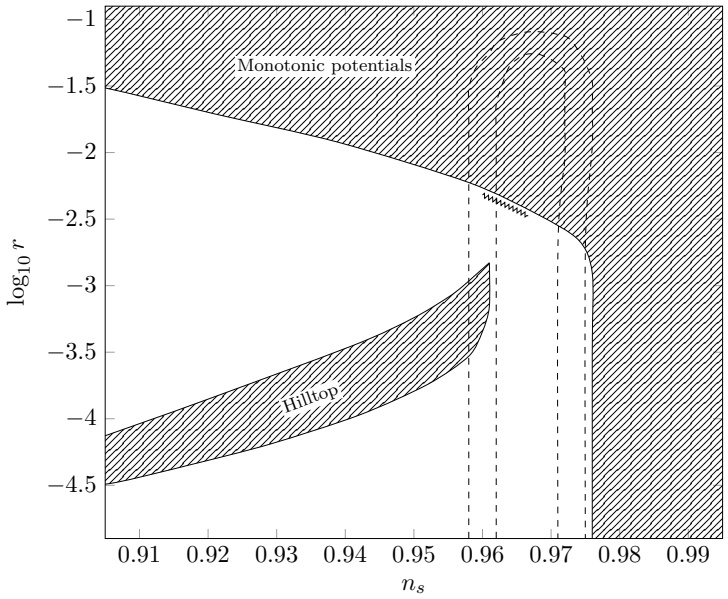

Figure 4.2: Predictions of Higgs inflation with quantum corrections calculated by the method presented in section 3.2.1. Shaded regions represent the allowed parameter space for the spectral index n_s and the tensor-to-scalar ratio r. The dashed lines give the one and two sigma measurement results of Planck combined with other cosmological data sets [18]. The zigzag line gives the tree-level predictions (4.4) for $N = 50 \ldots 60$. Results for the monotonic potentials are extrapolated from [65], figure 1; they should be compared to the hilltop results from [1], which occupy an otherwise excluded region of the parameter space. In particular, for smaller r values around $r \sim 10^{-4} \ldots 10^{-3}$, hilltop potentials are more compatible with the Planck results than the monotonic potentials.

of the hilltop. They form a raising curve in the $(r,\ n_s)$ plane with

$$n_s < 1 - \frac{2}{N}\,, \qquad r < \frac{3}{N^2}\,, \tag{4.7}$$

where the maximum values are reached when the hilltop is pushed to infinitely large field values. There n_s agrees with the tree-level prediction (4.4), but, remarkably, r is always at least four times smaller than in the tree-level case. This property is retained in the numerical analysis with the full quantum-corrected potential described in section 3.2.1. Hilltop potentials open up a section of the space of allowed CMB observables that can't be reached at tree level or with the features of the previous section, see figure 4.2.

4.4 Palatini Higgs inflation

The above analysis can be repeated in a straightforward manner in the Palatini formulation of section 3.2.3. Due to the different relations between χ and ξ, compare (3.27) and (3.34), the results will be slightly different. At tree level [58],

$$n_s = 1 - \frac{2}{N}\,, \quad r = \frac{2}{\xi N^2}\,, \quad \alpha_s = -\frac{2}{N^2}\,, \quad \beta_s = -\frac{4}{N^3}\,, \quad A_s = \frac{\lambda N^2}{12\pi^2\xi}\,, \tag{4.8}$$

compare to (4.4). The condition for A_s gives $\xi \approx 3.8 \times 10^6 \lambda N^2$, which is typically bigger than in the metric case: for $\lambda \sim 0.1$, we need $\xi \sim 10^9$. In leading slow-roll order, predictions for n_s, α_s, and β_s are the same for both the metric and Palatini cases, but r is heavily suppressed by the large ξ. Quantum corrections to the tree-level results have been worked out in [1, 67], and in all cases, r is small enough to be undetectable in CMB experiments in the foreseeable future. This is the main difference and discerning factor between the metric and Palatini Higgs inflation scenarios.

4.5 Other extensions

There are many ways to extend the simple single field Higgs inflation scenario presented in this chapter. One can, for example, add an R^2 term into the gravity part of the action [71–73], which modifies the results. The R^2 term alone produces the Starobinsky inflation [74], whose tree-level CMB predictions are equal to the tree-level Higgs case [75]. Both the tree-level Higgs inflation and the Starobinsky inflation belong to a more general class of inflationary models called α-attractors [76–78] with similar CMB predictions in terms of the number of e-folds N. In the Palatini formulation, new terms containing the covariant derivative of the metric may also be added to the action [79].

In the following chapters, we stick with the simple single-field Higgs inflation described here and study its phenomenology further.

Chapter 5

Reheating

After cosmic inflation ends, the universe must transition to the well-studied radiation-dominated stage. The transition process is called reheating. During reheating, the inflaton field typically oscillates around its vacuum value, and its interactions with the SM fields induce production of SM particles. This drains energy from the inflaton condensate and transfers it to the particles, which eventually come to dominate the energy density, thermalize, and usher in the hot radiation-dominated era.

In this chapter, we consider reheating in Higgs inflation. We go through the dominant reheating processes in the metric formulation of general relativity, and explain how they change in the Palatini formulation.

5.1 The reheating process

During slow-roll inflation, the inflaton field rolls towards a minimum of the potential. To have a graceful exit from inflation, the SR conditions (2.9) and (2.10) must be broken before the minimum is reached, and inflation ends. The field value starts to oscillate around the minimum, still following the field equation (2.8)

$$\ddot{\phi} + 3H\dot{\phi} + V'(\phi) = 0\,. \tag{5.1}$$

For example, for a quartic potential $V(\phi) = \frac{1}{2}m^2\phi^2$, neglecting the friction term $3H\dot{\phi}$ caused by expansion of space, the solution of (5.1) is a sinusoidally oscillating field with $\phi \propto \sin(mt)$.

The friction term decreases the oscillation amplitude. If left undisturbed, the oscillations eventually die away, and the inflaton relaxes to its vacuum value, resulting in an empty universe. However, in practice, the oscillation of the homogeneous inflaton field induces particle production in both the inflaton and other fields, so that part of the energy density of the inflaton condensate is transferred into a bath of particles.

5.1.1 Particle production

There are two ways to produce particles during reheating. Originally, direct particle decay was considered [80]: the homogeneous, oscillating inflaton field may be interpreted as a collection of inflaton particles with zero momenta and coherent phases. These particles then decay perturbatively into particles of other fields that interact with the inflaton; decay rates can be calculated by the usual quantum field theory methods.

In addition, there is another mechanism for particle production called *preheating* [81]. In preheating, particles are produced non-perturbatively, through a time-dependent mass term that originates from the oscillating inflaton condensate. As an example, let's consider the production of particles of a scalar field σ. The inflaton ϕ is coupled to σ through an interaction term $\frac{1}{2}\sigma^2 m^2(\phi)$, and the Fourier mode functions of σ follow the equations of motion

$$\ddot{\sigma}_k + 3H\dot{\sigma}_k + \omega_k^2 \sigma_k^2 = 0\,, \qquad \omega_k^2 \equiv \frac{k^2}{a^2} + m^2(\phi)\,, \tag{5.2}$$

where we neglected all other interactions as perturbative corrections. If the mass factor m is constant or changes slowly, then the solution of (5.2) for sub-Hubble scales is simply a linear combination of two oscillating modes:

$$a^{3/2}(t)\sigma_k(t) = \frac{\alpha_k}{\sqrt{2\omega_k(t)}} e^{-i\int^t \omega_k(t')\,dt'} + \frac{\beta_k}{\sqrt{2\omega_k(t)}} e^{i\int^t \omega_k(t')\,dt'} \tag{5.3}$$

with the normalization condition $|\alpha_k|^2 - |\beta_k|^2 = 1$ [82]. For the adiabatic vacuum, $\alpha_k = 1$ and $\beta_k = 0$; if there are particles present, their number density is given by

$$n_k = |\beta_k|^2\,. \tag{5.4}$$

As long as the mass changes slowly, (5.3) applies and n_k stays constant. However, if it changes quickly, the adiabaticity condition

$$\left|\frac{\dot{\omega}_k}{\omega_k^2}\right| \ll 1 \tag{5.5}$$

is broken, the solution to (5.2) is more complicated, (5.3) does not apply, and the particle concept becomes ill-defined. If adiabaticity is later restored, the new values of α_k and β_k may differ from the original ones, that is, production or destruction of particles may take place during the non-adiabatic period.

For a mass term produced by an oscillating inflaton field with $m \to 0$ at the bottom of the inflaton potential (say, $m \propto \phi^n$ with a minimum at $\phi = 0$), the adiabaticity condition (5.5) applies for sub-Hubble modes at large field values, but is broken when the inflaton crosses the minimum. Efficient particle production can take place there if the oscillations of the mass term are properly 'in sync' with the natural oscillation frequency of the mode. The situation is analogous to a driven oscillator where the mass term provides the driving force, and a proper driving frequency amplifies the mode amplitude. This is called parametric resonance, and it leads to the formation of resonance bands for certain k-values where particle production is most

efficient [81–86]. When the expansion of space is taken into account, the redshift of momenta moves the modes on and off the resonance bands resulting in stochastic effects [82]. Details of this process must be worked out separately for each model to obtain the efficiency of particle production through this channel.

In addition to parametric resonance, non-perturbative particle production can proceed through tachyonic preheating [87, 88]. There the mass squared in (5.2) is negative, which results in the exponential growth of certain mode functions and a rapid increase in the energy density of the perturbations. This happens, for example, if the mass term of the inflaton field itself given by $m^2 = V''(\phi)$ is negative at some point during the inflaton oscillation. We will see in section 5.2.2 that tachyonic preheating can be highly efficient.

In practice, particle production during reheating is a combination of preheating and perturbative decays. Preheating is typically more important in the early stages of particle production (hence the name) and particle decays take over later.

5.2 Higgs reheating

In Higgs inflation with a non-minimal coupling to gravity, the above principles of inflaton oscillation and particle production all come into play. Inflation ends when the SR conditions break at $h \sim 1/\sqrt{\xi}$, and after this, the Higgs field starts to oscillate around $h = 0$. The oscillating field gives masses to fermions, massive gauge bosons and the Higgs boson itself through the potential and mass terms (3.26) and (3.29), so these particles can be produced in preheating. In addition, perturbative Higgs decays need to be considered. We next describe how reheating proceeds in the metric formulation of the model [89–96], and then proceed to the Palatini formulation, which was analyzed in the second article of this thesis [2].

5.2.1 Metric formulation: combined preheating

In the metric formulation, at $1/\xi \lesssim h \lesssim 1/\sqrt{\xi}$, we get from (3.26)

$$V_E(\chi) \approx \frac{1}{2} M_\chi^2 \chi^2 \,, \qquad M_\chi^2 \equiv \sqrt{\frac{\lambda}{3\xi^2}} \,, \tag{5.6}$$

that is, the Einstein frame potential for the canonical field χ is approximately quadratic. The field oscillates sinusoidally, but the oscillation amplitude decreases quickly due to the expansion of space. The Higgs boson mass M_χ^2 is initially small compared to the masses of other particles, so particle production through perturbative decay of the condensate is not possible. The mass is also constant, so Higgs bosons are not produced in preheating, but other massive particles can be. Direct fermion production is suppressed by Pauli blocking, but massive gauge bosons $W^\pm$ and Z are produced efficiently. However, the gauge bosons quickly decay into fermions through perturbative channels. The result is *combined preheating* [89], where at each Higgs field oscillation, $W^\pm$ and Z bosons are produced at the zero crossing of χ, and they decay

almost completely into fermions during the next semi-oscillation, until more gauge bosons are produced at the next zero crossing. Effectively, energy is 'pumped' from the Higgs condensate into fermions. Eventually, the Higgs oscillation amplitude decays and the gauge boson masses decrease enough to suppress the decay, and gauge bosons start to accumulate through parametric resonance. This quickly depletes the condensate and leads to a radiation-dominated universe which thermalizes to a high temperature. The transition from inflation to radiation domination takes a few e-folds.

There is potentially an additional particle production channel in the metric formulation of Higgs inflation: the would-be Goldstone bosons, or equivalently, longitudinal gauge bosons, can be produced violently near the zero crossing of χ due to a 'spike' in the internal metric of the Higgs doublet in the Einstein frame [92–96]. This could lead to a quicker reheating than the above described combined preheating process; however, the validity of this analysis was questioned in [2], since the energy of the produced particles seems to exceed the cut-off scale of the model. This spike is not present in the Palatini formulation [2]. In any case, successful reheating, and a graceful exit from inflation to early radiation domination, is expected in the metric formulation of Higgs inflation.

5.2.2 Palatini formulation: tachyonic preheating

Preheating in the Palatini formulation of Higgs inflation was studied in detail in the second article of this thesis [2]. In the Palatini formulation, the Einstein frame potential is different from the metric one, and this leads to drastic changes in the preheating phase. In particular, the oscillation amplitude decays much slower in the Palatini formulation, so χ returns to the inflationary plateau at $h \sim 1/\sqrt{\xi}$ after every semi-oscillation. We can understand this difference by comparing the relations between χ and h in the two formulations. The energy of the oscillations, proportional to the oscillation amplitude, is given by the Hubble parameter H in the Friedmann equations (2.7). The change of H in terms of h may be written as

$$\frac{dH}{dh} = -\frac{\dot{\chi}^2}{2\dot{h}} = -\frac{1}{2}\sqrt{6H^2 - 2V_E[\chi(h)]}\frac{d\chi}{dh}\,, \tag{5.7}$$

where we used the Friedmann and scalar field equations (2.7) and (2.8). In both formulations, inflation ends at $h \sim 1/\sqrt{\xi}$, so the change of h from the end of inflation to the first zero crossing is the same. Potential V_E also has the same form in terms of h. However, $\frac{d\chi}{dh}$ in (5.7) is always bigger in the metric formulation, compare (3.24) to (3.33), so in the metric formulation H decreases much more before the first zero crossing. This explains why the oscillation amplitude decays fast in the metric formulation, while it stays almost constant in the Palatini case.

This new background dynamic has a drastic effect on preheating: while the combined preheating process mentioned above still works, the leading preheating channel is tachyonic Higgs production. Near the plateau, the Higgs boson mass V_E'' is negative, see figure 5.1, and since the field returns there over and over again, this leads to explosive enhancement of the Higgs perturbations, as discussed in section 5.1.1. As a result, the universe transitions from inflation

to radiation domination very quickly, in less than one e-fold. We conclude that reheating in Palatini Higgs inflation is practically instantaneous.

5.3 Observational significance

For an inflationary model to be successful, it is important to know that reheating works in the model, that is, the universe can transition to radiation domination with a high enough temperature for all well-known early-time phenomenology, such as primordial nucleosynthesis and recombination. In addition, detailed knowledge of the reheating process is interesting because it affects the CMB predictions of the model. Different durations of reheating translate into different numbers of e-folds N needed between the Hubble exit of the CMB pivot scale and the end of inflation, and this affects model predictions for observables like n_s and r. In particular, in Higgs inflation, the leading n_s prediction (4.4) changes in terms of N as

$$dn_s = \frac{2}{N^2} dN \sim 10^{-3} dN \tag{5.8}$$

for $N \sim 50$. We see that order one changes in N correspond to changes of order 10^{-3} in n_s. This is the accuracy of the current and future CMB observations (2.21). To get most out of the observations, and to differentiate between different models such as the metric and Palatini formulations of Higgs inflation or the extensions mentioned in section 4.5, predictions need to be made with this accuracy, and for this we need higher-order corrections to the standard calculation, including accurate knowledge on reheating dynamics and N.

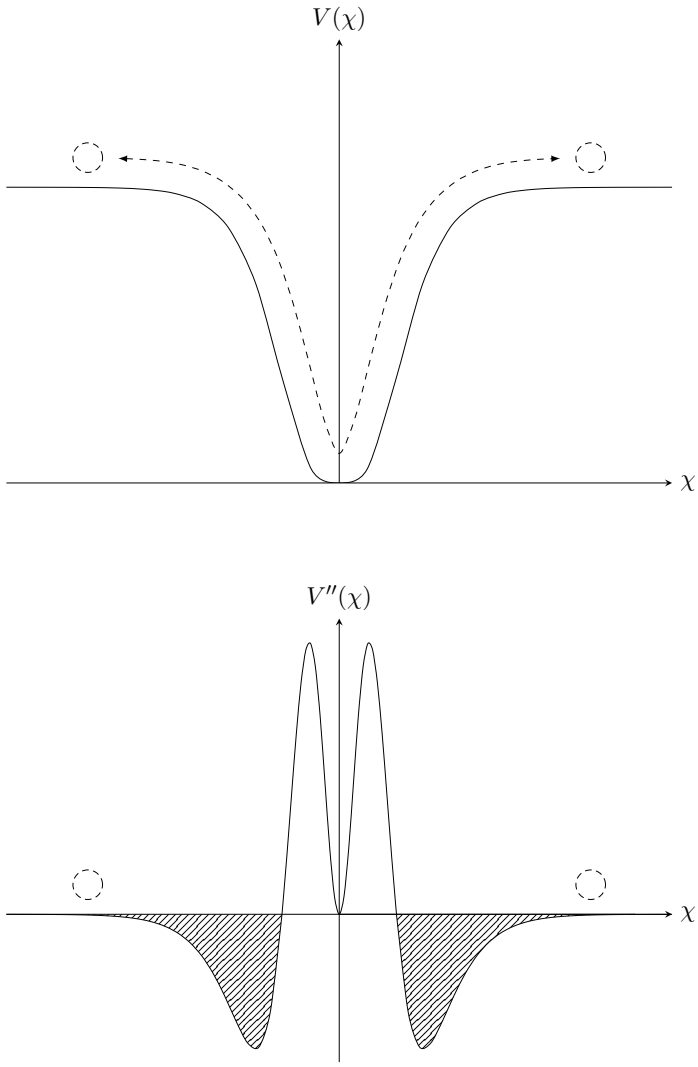

Figure 5.1: Preheating in Palatini Higgs inflation. Top: Einstein frame Higgs potential in the Palatini formalism. Bottom: second derivative of the potential, that is, the mass squared of the Higgs perturbations at a given background field value, with shaded tachyonic regions. During preheating, the background field oscillates in the potential well. The dashed circles denote a typical oscillation amplitude. During the oscillation, the background field repeatedly returns to the tachyonic region, and this leads to violent amplification of the Higgs perturbations.

Chapter 6

Primordial black holes

Astrophysical black holes are dense objects formed from collapsing stars. However, black hole formation is also possible through other processes, in particular in the high energy density conditions of the early universe. Such primordial black holes (PBHs) may be formed, for example, from strong inflationary perturbations. The study of PBHs is interesting since they could constitute all or part of the dark matter, and it may be possible to detect them in upcoming gravitational wave experiments.

In this chapter, we discuss the formation of PBHs from inflation. We show that the strong perturbations needed can be obtained from a feature in the inflaton potential, and consider the prospects of PBH dark matter in Higgs inflation.

6.1 PBH formation

As discussed in section 2.3, curvature perturbations on super-Hubble scales freeze to constant values. Expansion of space is fast enough to resist gravitational collapse at these scales. However, after inflation, the expansion rate starts to decrease and comoving scales begin to re-enter the Hubble radius. Perturbations start to grow, and the densest regions may even collapse into primordial black holes [97, 98].

Let us look at perturbation modes with wavenumber k that during inflation left the Hubble radius ΔN e-folds after the CMB pivot scale k_* (then $\Delta N \lesssim 50$). When this scale re-enters the Hubble radius after inflation, a PBH formed by it will contain roughly all matter in one Hubble patch, so its mass is [3, 98]

$$M_{\mathrm{PBH}} = \gamma \frac{4\pi}{3} H^{-3} \rho \approx 2 \times 10^{15} \times e^{-2\Delta N} M_\odot \,, \tag{6.1}$$

where $M_\odot$ is the solar mass, γ is an efficiency factor, and in the last step we assumed a radiation-dominated universe with $\gamma \approx 0.2$ [98]. As time goes on, scales closer to k_* start to enter the Hubble radius, so ΔN decreases and the mass of the formed PBHs increases. All PBHs compatible with cosmological observations form deep in the radiation-dominated era—PBHs formed at later times would be heavier than the mass scale of galaxies.

To estimate the abundance of the PBHs, we can approximate their formation to follow Gaussian statistics with a variance of order $\mathcal{P}_\mathcal{R}(k)$ [98–100]. PBHs are then formed for perturbations that exceed a threshold value ζ_c, estimated by analytical and numerical calculations to be $\zeta_c = 0.07 \ldots 1.3$ [98, 100–105]. The formed PBHs move at non-relativistic velocities, so their combined energy density scales as a^{-3} as the universe expands, whereas the radiation energy density scales as a^{-4}. Thus the energy density fraction in the PBHs grows over time. Combining all these factors, the PBH energy density fraction at the time of matter radiation equality can be expressed as [3]

$$\Omega_{\mathrm{PBH\,eq}} \propto e^{-\frac{\zeta_c^2}{2\mathcal{P}_\mathcal{R}(k)}+\Delta N}, \tag{6.2}$$

where we neglected a prefactor that is insignificant compared to the exponent. Since $\Delta N \lesssim 50$, taking into account the estimates for ζ_c above, if we want PBHs to constitute a significant part of the matter content of the universe, say $\Omega_{\mathrm{PBH\,eq}} = 0.1 \ldots 0.5$, we need at least $\mathcal{P}_\mathcal{R}(k) \gtrsim 10^{-4}$.

The analysis leading to (6.2) contains many uncertainties. The exact value of ζ_c is one of these; other issues include the correct choice of window function for the perturbations [106], differences arising from a calculation scheme based on peaks theory [99, 100, 107, 108], the effect of possible non-Gaussianities [109, 110] and quantum diffusion [110–115], and the need to integrate over PBHs formed on different scales k. However, (6.2) may still be used as an order-of-magnitude estimate: significant amounts of PBHs on some scale are formed only if the super-Hubble curvature power spectrum reaches the value 10^{-4} there.

6.2 PBHs as dark matter

If a significant amount of PBHs is formed in the early universe, they could constitute all or part of the dark matter [97, 116]. However, black hole dark matter is severely restricted by observations on gravitational lensing, gamma ray background, accretion and various other dynamical and large-scale structure constraints [117–119], see figure 6.1. There are still two mass windows where all dark matter could be in the form of PBHs: solar mass black holes with $M = 25 \ldots 100 M_\odot$, or lighter ones with $M = 3.5 \times 10^{-17} \ldots 4 \times 10^{-12} M_\odot = 7 \times 10^{16} \ldots 8 \times 10^{21}$ g [119, 120].

There is one way to get around the constraints. Black holes slowly evaporate their energy away through Hawking radiation [126], and PBHs with an initial mass below 10^{15} g would have had enough time to disappear completely by now. However, it is possible that the evaporation stops before all of the black hole's mass has vanished, leaving behind light relics of, say, the Planck mass [127–129]. If the initial mass of a PBH is less than 10^6 g, then it evaporates early enough to not violate any observational constraints, and Planck mass relics from such PBHs could constitute all of the dark matter [130–135].

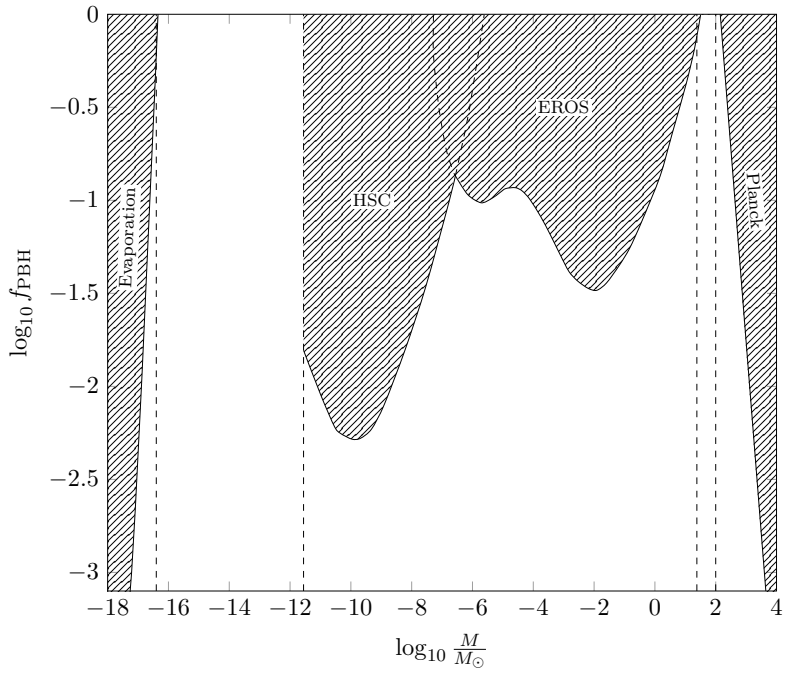

Figure 6.1: Observational limits for PBH abundance if PBHs only form on one mass scale. The image is adapted from figure 1 in [119], but we have ignored all subdominant and uncertain limits, in particular in the low mass range [120–122]. Here M is the mass of the black holes, and f_{PBH} is the fraction of dark matter that consists of PBHs. Shaded regions are excluded by the effects of black hole evaporation on the Big Bang nucleosynthesis and the extragalactic photon background [117], the expected gravitational microlensing from the PBHs (from two different experiments, HSC [123] and EROS [124]), and radiation from matter that is accreted around PBHs and could change the Planck CMB observations [125]. There are two windows where PBHs could still make up all or almost all of the dark matter: $M = 3.5 \times 10^{-17} \ldots 4 \times 10^{-12} M_\odot$ and $M = 25 \ldots 100 M_\odot$. At the time of writing, the literature on the constraints is evolving rapidly, and the figure should be understood as a sketch only; this will not affect our conclusions in section 6.3.1.

6.3 PBH dark matter from inflation

The super-Hubble curvature perturbations that later collapse into black holes are formed during inflation, so we can use the standard perturbation theory analysis of section 2.3 to analyse PBH formation in a given inflationary model. Note that at the CMB pivot scale, $\mathcal{P}_\mathcal{R}(k_*) \approx 2.1 \times 10^{-9}$ (2.20), which is too small for abundant PBH formation. Also, according to (6.1), k_* corresponds to PBHs with mass $10^{15}\ M_\odot$, which are too heavy to constitute the observed dark matter. In practice, dark matter PBHs must form on scales that exit the Hubble radius later than k_*, and the power spectrum there must take the high value $\mathcal{P}_\mathcal{R} \gtrsim 10^{-4}$ mentioned earlier.

In SR inflation discussed in section 2.2.1, a high $\mathcal{P}_\mathcal{R}$ value is achieved for small ϵ_V, see equation (2.23), that is, in a flat region in the inflationary potential. However, an extended flat region in the potential may lead to a too high number of e-folds of inflation between the Hubble exit of the pivot scale k_* and the end of inflation, as can be seen from (2.14). In practice, successful PBH formation requires that ϵ_V is small only for a small field range and grows on either side, corresponding to a (near-)critical point where η_V is also small or vanishing. PBHs are then formed by a local feature in the potential that resembles those discussed in section 4.3.1 and depicted on the left-hand side of figure 4.1. Such models were originally studied in [136–140], and more recently in [105, 141–146] after the renewed interest in PBHs due to the detection of gravitational waves from merging black holes by LIGO and Virgo [147].

Note that if ϵ_V becomes very small so that $V' \to 0$, the field equation (2.8) approaches the form

$$\ddot{\phi} + 3H\dot{\phi} = 0\,. \tag{6.3}$$

For this equation, the SR condition $|\eta_H| < 1$ (2.10) fails, and thus also the result (2.23) for $\mathcal{P}_\mathcal{R}$ becomes unreliable [105, 143, 144, 146, 148]. Equation (6.3) describes *ultra-slow-roll inflation* [113, 149–152], where the field velocity decreases exponentially:

$$\dot{\phi} \propto e^{-3Ht} \propto a^{-3}\,. \tag{6.4}$$

For the perturbations, this leads to an exponential growth and an enhancement of $\mathcal{P}_\mathcal{R}(k)$ even on super-Hubble scales [3, 150], since in the expression (2.17) for $\mathcal{P}_\mathcal{R}(k)$,

$$\mathcal{P}_\mathcal{R}(k) = \frac{k^3}{2\pi^2}\frac{|\mu_k|^2}{z^2}\,, \tag{6.5}$$

the factor $z = a\frac{\dot{\phi}}{H} \propto a^{-2}$ decreases rapidly. In other words, even though the SR approximation may fail near a critical point, an enhancement of the power spectrum is expected there. However, to calculate $\mathcal{P}_\mathcal{R}(k)$ outside of SR, the mode equations (2.15) need to be solved numerically on a case-by-case basis.

6.3.1 Higgs inflation

PBH production in the non-minimally coupled Higgs inflation was first considered in [142], where the authors found solutions that permitted the production of PBHs in the SR approximation, but

they used an unrealistically strong phenomenological running of the non-minimal coupling ξ. In [3], the third paper of this thesis, PBH production in Higgs inflation was studied in detail, with the quantum-corrected potential introduced in section 3.2.1, by scanning over all appropriate critical and near-critical point potentials and calculating the produced power spectra $\mathcal{P}_\mathcal{R}(k)$ numerically.

It was found that PBHs can indeed be produced in large abundances by fine-tuning the model parameters. Strongest PBH production occurs when the potential has a local minimum at the PBH scale. The SR approximation breaks down before the field reaches the minimum, but the field returns to SR inflation once it has passed the subsequent local potential maximum. Perturbations are strongly enhanced in the intermediary region. Both the abundance and mass of the formed PBHs can be tuned freely in the model.

However, there emerges a correlation between the PBH mass M and the spectral index n_s at k_*, see figure 6.2. In particular, to satisfy the observational constraints on n_s (2.21), the mass needs to be less than 10^6 g. As discussed in section 6.1, such light PBHs would have evaporated completely by now—unless they leave behind Planck mass relics. If the relic hypothesis is correct, then Higgs inflation can produce the correct abundance of dark matter in the form of these relics.

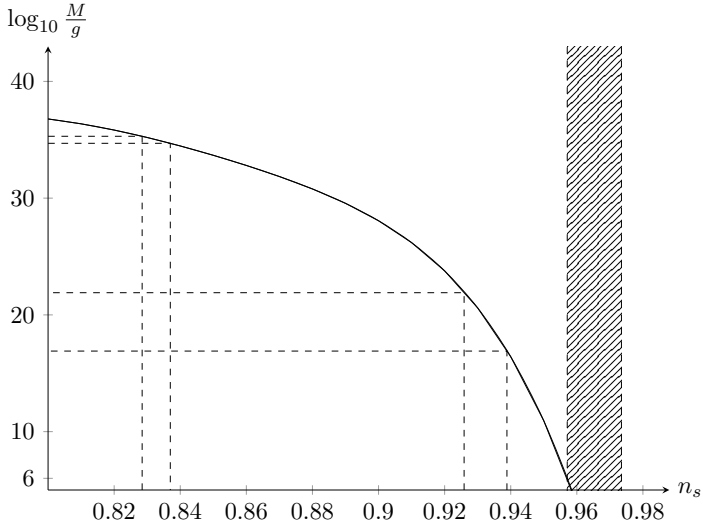

Figure 6.2: Correlation between the PBH mass M and the CMB spectral index n_s in Higgs inflation, adapted from figure 9 in [3]. The solid line gives the allowed (n_s, M) values and the dashed lines indicate the allowed PBH mass windows from figure 6.1. The n_s region allowed by Planck [18] is shaded and is not compatible with the PBH windows. However, PBHs with initial masses $M < 10^6$ g evaporate early enough to evade the observational black hole limits, are compatible with the CMB, and could leave behind Planck mass relics as dark matter.

Chapter 7

Conclusions and outlook

In this thesis, we have seen how the Standard Model Higgs field can drive inflation, and what cosmological repercussions this may have. Despite its simplicity, Higgs inflation is a flexible cosmological model, which can be extended and fine-tuned to produce a wide variety of scenarios with different observational signatures.

In the papers included in this thesis, we have studied a few such scenarios. In hilltop Higgs inflation, we found out that the predicted tensor-to-scalar ratio is $r \lesssim 1.2 \times 10^{-3}$, that is, smaller by at least a factor of four compared to the tree-level prediction. In reheating, we saw that the transition from inflation to radiation domination is much faster in the Palatini formulation of general relativity compared to the usual metric one, and this affects the spectral index n_s at the level of 10^{-3}, which is probed by future CMB experiments. This also shows that cosmological observations concerning the early times of the universe have the power to distinguish between different formulations of general relativity which may be indistinguishable in today's universe. We also saw that with sufficient fine-tuning, primordial black holes can be produced abundantly in Higgs inflation, although their mass must be small to also match the CMB measurements. Nevertheless, these black holes may constitute the dark matter if they leave behind Planck mass relics as they evaporate. Remarkably, all this can be achieved without adding any new fields to the standard model of particle physics.

All these studies would be of questionable value if they could not be compared to current or future experimental data. Fortunately, observational cosmology is going strong. Results of the Planck satellite [153] already constrain the CMB observables to a high degree, and other surveys will provide even better data in the future. In particular, the BICEP and Keck Array aim to detect or rule out the tensor-to-scalar ratio at the level of $r \sim 0.005$ in the near future [154], and the Simons Observatory [155] aims to push this down to $r \sim 0.003$ [156]. At the same time, the large-scale structure will be probed more accurately by the Euclid satellite [157, 158]. These developments promise fruitful times ahead for the cosmology of the early universe.

Bibliography

[1] V.-M. Enckell, K. Enqvist, S. Rasanen and E. Tomberg, *Higgs inflation at the hilltop*, *JCAP* **1806** (2018) 005, [1802.09299].

[2] J. Rubio and E. S. Tomberg, *Preheating in Palatini Higgs inflation*, *JCAP* **1904** (2019) 021, [1902.10148].

[3] S. Rasanen and E. Tomberg, *Planck scale black hole dark matter from Higgs inflation*, *JCAP* **1901** (2019) 038, [1810.12608].

[4] S. M. Carroll, *Spacetime and geometry: An introduction to general relativity*. 2004.

[5] D. H. Lyth and A. R. Liddle, *The primordial density perturbation: Cosmology, inflation and the origin of structure*. 2009.

[6] D. Kazanas, *Dynamics of the Universe and Spontaneous Symmetry Breaking*, *Astrophys. J.* **241** (1980) L59–L63.

[7] A. H. Guth, *The Inflationary Universe: A Possible Solution to the Horizon and Flatness Problems*, *Phys. Rev.* **D23** (1981) 347–356.

[8] K. Sato, *Cosmological Baryon Number Domain Structure and the First Order Phase Transition of a Vacuum*, *Phys. Lett.* **99B** (1981) 66–70.

[9] A. D. Linde, *A New Inflationary Universe Scenario: A Possible Solution of the Horizon, Flatness, Homogeneity, Isotropy and Primordial Monopole Problems*, *Phys. Lett.* **108B** (1982) 389–393.

[10] A. Albrecht and P. J. Steinhardt, *Cosmology for Grand Unified Theories with Radiatively Induced Symmetry Breaking*, *Phys. Rev. Lett.* **48** (1982) 1220–1223.

[11] A. D. Linde, *Chaotic Inflation*, *Phys. Lett.* **129B** (1983) 177–181.

[12] A. R. Liddle, P. Parsons and J. D. Barrow, *Formalizing the slow roll approximation in inflation*, *Phys. Rev.* **D50** (1994) 7222–7232, [astro-ph/9408015].

[13] V. F. Mukhanov, H. A. Feldman and R. H. Brandenberger, *Theory of cosmological perturbations. Part 1. Classical perturbations. Part 2. Quantum theory of perturbations. Part 3. Extensions*, *Phys. Rept.* **215** (1992) 203–333.

[14] V. F. Mukhanov, *Quantum Theory of Gauge Invariant Cosmological Perturbations*, *Sov. Phys. JETP* **67** (1988) 1297–1302.

[15] N. D. Birrell and P. C. W. Davies, *Quantum Fields in Curved Space*. Cambridge Monographs on Mathematical Physics. Cambridge Univ. Press, Cambridge, UK, 1984, 10.1017/CBO9780511622632.

[16] K. A. Malik and D. Wands, *Cosmological perturbations*, *Phys. Rept.* **475** (2009) 1–51, [0809.4944].

[17] D. H. Lyth, K. A. Malik and M. Sasaki, *A General proof of the conservation of the curvature perturbation*, *JCAP* **0505** (2005) 004, [astro-ph/0411220].

[18] Planck collaboration, Y. Akrami et al., *Planck 2018 results. X. Constraints on inflation*, 1807.06211.

[19] BICEP2, Keck Array collaboration, P. A. R. Ade et al., *BICEP2 / Keck Array x: Constraints on Primordial Gravitational Waves using Planck, WMAP, and New BICEP2/Keck Observations through the 2015 Season*, *Phys. Rev. Lett.* **121** (2018) 221301, [1810.05216].

[20] Planck collaboration, P. A. R. Ade et al., *Planck 2013 results. XXII. Constraints on inflation*, *Astron. Astrophys.* **571** (2014) A22, [1303.5082].

[21] Particle Data Group collaboration, M. Tanabashi et al., *Review of Particle Physics*, *Phys. Rev.* **D98** (2018) 030001.

[22] J. Erler and M. Schott, *Electroweak Precision Tests of the Standard Model after the Discovery of the Higgs Boson*, *Prog. Part. Nucl. Phys.* **106** (2019) 68–119, [1902.05142].

[23] S. Weinberg, *The Quantum theory of fields. Vol. 1: Foundations*. Cambridge University Press, 2005.

[24] S. Weinberg, *The quantum theory of fields. Vol. 2: Modern applications*. Cambridge University Press, 2013.

[25] M. E. Peskin and D. V. Schroeder, *An Introduction to quantum field theory*. Addison-Wesley, Reading, USA, 1995.

[26] S. R. Coleman and E. J. Weinberg, *Radiative Corrections as the Origin of Spontaneous Symmetry Breaking*, *Phys. Rev.* **D7** (1973) 1888–1910.

[27] C. Ford, D. R. T. Jones, P. W. Stephenson and M. B. Einhorn, *The Effective potential and the renormalization group*, *Nucl. Phys.* **B395** (1993) 17–34, [hep-lat/9210033].

[28] J. Fumagalli and M. Postma, *UV (in)sensitivity of Higgs inflation*, *JHEP* **05** (2016) 049, [1602.07234].

[29] M. Atkins and X. Calmet, *Bounds on the Nonminimal Coupling of the Higgs Boson to Gravity*, *Phys. Rev. Lett.* **110** (2013) 051301, [1211.0281].

[30] J. Ren, Z.-Z. Xianyu and H.-J. He, *Higgs Gravitational Interaction, Weak Boson Scattering, and Higgs Inflation in Jordan and Einstein Frames*, *JCAP* **1406** (2014) 032, [1404.4627].

[31] F. L. Bezrukov and M. Shaposhnikov, *The Standard Model Higgs boson as the inflaton*, *Phys. Lett.* **B659** (2008) 703–706, [0710.3755].

[32] F. Bezrukov and M. Shaposhnikov, *Standard Model Higgs boson mass from inflation: Two loop analysis*, *JHEP* **07** (2009) 089, [0904.1537].

[33] F. Feruglio, *The Chiral approach to the electroweak interactions*, *Int. J. Mod. Phys.* **A8** (1993) 4937–4972, [hep-ph/9301281].

[34] F. L. Bezrukov, A. Magnin and M. Shaposhnikov, *Standard Model Higgs boson mass from inflation*, *Phys. Lett.* **B675** (2009) 88–92, [0812.4950].

[35] S. Dutta, K. Hagiwara, Q.-S. Yan and K. Yoshida, *Constraints on the electroweak chiral Lagrangian from the precision data*, *Nucl. Phys.* **B790** (2008) 111–137, [0705.2277].

[36] F. Bezrukov, A. Magnin, M. Shaposhnikov and S. Sibiryakov, *Higgs inflation: consistency and generalisations*, *JHEP* **01** (2011) 016, [1008.5157].

[37] D. P. George, S. Mooij and M. Postma, *Quantum corrections in Higgs inflation: the real scalar case*, *JCAP* **1402** (2014) 024, [1310.2157].

[38] F. Bezrukov and M. Shaposhnikov, *Higgs inflation at the critical point*, *Phys. Lett.* **B734** (2014) 249–254, [1403.6078].

[39] F. Bezrukov, J. Rubio and M. Shaposhnikov, *Living beyond the edge: Higgs inflation and vacuum metastability*, *Phys. Rev.* **D92** (2015) 083512, [1412.3811].

[40] D. P. George, S. Mooij and M. Postma, *Quantum corrections in Higgs inflation: the Standard Model case*, *JCAP* **1604** (2016) 006, [1508.04660].

[41] J. Weenink and T. Prokopec, *Gauge invariant cosmological perturbations for the nonminimally coupled inflaton field*, *Phys. Rev.* **D82** (2010) 123510, [1007.2133].

[42] X. Calmet and T.-C. Yang, *Frame Transformations of Gravitational Theories*, *Int. J. Mod. Phys.* **A28** (2013) 1350042, [1211.4217].

[43] C. F. Steinwachs and A. Yu. Kamenshchik, *Non-minimal Higgs Inflation and Frame Dependence in Cosmology*, *AIP Conf. Proc.* **1514** (2013) 161–164, [1301.5543].

[44] A. Yu. Kamenshchik and C. F. Steinwachs, *Question of quantum equivalence between Jordan frame and Einstein frame*, *Phys. Rev.* **D91** (2015) 084033, [1408.5769].

[45] Y. Hamada, H. Kawai, Y. Nakanishi and K.-y. Oda, *Meaning of the field dependence of the renormalization scale in Higgs inflation*, *Phys. Rev.* **D95** (2017) 103524, [1610.05885].

[46] M. Postma and M. Volponi, *Equivalence of the Einstein and Jordan frames*, *Phys. Rev.* **D90** (2014) 103516, [1407.6874].

[47] C. P. Burgess, H. M. Lee and M. Trott, *Power-counting and the Validity of the Classical Approximation During Inflation*, *JHEP* **09** (2009) 103, [0902.4465].

[48] J. L. F. Barbon and J. R. Espinosa, *On the Naturalness of Higgs Inflation*, *Phys. Rev.* **D79** (2009) 081302, [0903.0355].

[49] M. P. Hertzberg, *On Inflation with Non-minimal Coupling*, *JHEP* **11** (2010) 023, [1002.2995].

[50] F. Bauer and D. A. Demir, *Higgs-Palatini Inflation and Unitarity*, *Phys. Lett.* **B698** (2011) 425–429, [1012.2900].

[51] X. Calmet and R. Casadio, *Self-healing of unitarity in Higgs inflation*, *Phys. Lett.* **B734** (2014) 17–20, [1310.7410].

[52] A. Escrivà and C. Germani, *Beyond dimensional analysis: Higgs and new Higgs inflations do not violate unitarity*, *Phys. Rev.* **D95** (2017) 123526, [1612.06253].

[53] G. Degrassi, S. Di Vita, J. Elias-Miro, J. R. Espinosa, G. F. Giudice, G. Isidori et al., *Higgs mass and vacuum stability in the Standard Model at NNLO*, *JHEP* **08** (2012) 098, [1205.6497].

[54] D. Buttazzo, G. Degrassi, P. P. Giardino, G. F. Giudice, F. Sala, A. Salvio et al., *Investigating the near-criticality of the Higgs boson*, *JHEP* **12** (2013) 089, [1307.3536].

[55] G. Iacobellis and I. Masina, *Stationary configurations of the Standard Model Higgs potential: electroweak stability and rising inflection point*, *Phys. Rev.* **D94** (2016) 073005, [1604.06046].

[56] A. Einstein, *Einheitliche Feldtheorie von Gravitation und Elektrizität*, *Sitzungber.Preuss.Akad.Wiss.* **22** (1925) 414–419.

[57] M. Ferraris, M. Francaviglia and C. Reina, *Variational formulation of general relativity from 1915 to 1925 "Palatini's method" discovered by Einstein in 1925*, *Gen.Rel.Grav.* **14** (1982) 243–254.

[58] F. Bauer and D. A. Demir, *Inflation with Non-Minimal Coupling: Metric versus Palatini Formulations*, *Phys. Lett.* **B665** (2008) 222–226, [0803.2664].

[59] J. W. York, Jr., *Role of conformal three geometry in the dynamics of gravitation*, *Phys. Rev. Lett.* **28** (1972) 1082–1085.

[60] G. W. Gibbons and S. W. Hawking, *Action Integrals and Partition Functions in Quantum Gravity*, *Phys. Rev.* **D15** (1977) 2752–2756.

[61] J. Rubio, *Higgs inflation*, *Front. Astron. Space Sci.* **5** (2019) 50, [1807.02376].

[62] Y. Hamada, H. Kawai and K.-y. Oda, *Minimal Higgs inflation*, *PTEP* **2014** (2014) 023B02, [1308.6651].

[63] K. Allison, *Higgs xi-inflation for the 125-126 GeV Higgs: a two-loop analysis*, *JHEP* **02** (2014) 040, [1306.6931].

[64] Y. Hamada, H. Kawai, K.-y. Oda and S. C. Park, *Higgs Inflation is Still Alive after the Results from BICEP2*, *Phys. Rev. Lett.* **112** (2014) 241301, [1403.5043].

[65] V.-M. Enckell, K. Enqvist and S. Nurmi, *Observational signatures of Higgs inflation*, *JCAP* **1607** (2016) 047, [1603.07572].

[66] F. Bezrukov, M. Pauly and J. Rubio, *On the robustness of the primordial power spectrum in renormalized Higgs inflation*, *JCAP* **1802** (2018) 040, [1706.05007].

[67] S. Rasanen and P. Wahlman, *Higgs inflation with loop corrections in the Palatini formulation*, *JCAP* **1711** (2017) 047, [1709.07853].

[68] A. Salvio, *Initial Conditions for Critical Higgs Inflation*, *Phys. Lett.* **B780** (2018) 111–117, [1712.04477].

[69] I. Masina, *Ruling out Critical Higgs Inflation?*, *Phys. Rev.* **D98** (2018) 043536, [1805.02160].

[70] L. Boubekeur and D. H. Lyth, *Hilltop inflation*, *JCAP* **0507** (2005) 010, [hep-ph/0502047].

[71] Y.-C. Wang and T. Wang, *Primordial perturbations generated by Higgs field and R^2 operator*, *Phys. Rev.* **D96** (2017) 123506, [1701.06636].

[72] Y. Ema, *Higgs Scalaron Mixed Inflation*, *Phys. Lett.* **B770** (2017) 403–411, [1701.07665].

[73] V.-M. Enckell, K. Enqvist, S. Rasanen and L.-P. Wahlman, *Higgs-R^2 inflation - full slow-roll study at tree-level*, 1812.08754.

[74] A. A. Starobinsky, *A New Type of Isotropic Cosmological Models Without Singularity*, *Phys. Lett.* **B91** (1980) 99–102.

[75] A. Kehagias, A. Moradinezhad Dizgah and A. Riotto, *Remarks on the Starobinsky model of inflation and its descendants*, *Phys. Rev.* **D89** (2014) 043527, [1312.1155].

[76] R. Kallosh and A. Linde, *Universality Class in Conformal Inflation*, *JCAP* **1307** (2013) 002, [1306.5220].

[77] R. Kallosh, A. Linde and D. Roest, *Superconformal Inflationary α-Attractors*, *JHEP* **11** (2013) 198, [1311.0472].

[78] M. Galante, R. Kallosh, A. Linde and D. Roest, *Unity of Cosmological Inflation Attractors*, *Phys. Rev. Lett.* **114** (2015) 141302, [1412.3797].

[79] S. Rasanen, *Higgs inflation in the Palatini formulation with kinetic terms for the metric*, 1811.09514.

[80] L. F. Abbott, E. Farhi and M. B. Wise, *Particle Production in the New Inflationary Cosmology*, *Phys. Lett.* **117B** (1982) 29.

[81] L. Kofman, A. D. Linde and A. A. Starobinsky, *Reheating after inflation*, *Phys. Rev. Lett.* **73** (1994) 3195–3198, [hep-th/9405187].

[82] L. Kofman, A. D. Linde and A. A. Starobinsky, *Towards the theory of reheating after inflation*, *Phys. Rev.* **D56** (1997) 3258–3295, [hep-ph/9704452].

[83] A. D. Dolgov and D. P. Kirilova, *ON PARTICLE CREATION BY A TIME DEPENDENT SCALAR FIELD*, *Sov. J. Nucl. Phys.* **51** (1990) 172–177.

[84] J. H. Traschen and R. H. Brandenberger, *Particle Production During Out-of-equilibrium Phase Transitions*, *Phys. Rev.* **D42** (1990) 2491–2504.

[85] Y. Shtanov, J. H. Traschen and R. H. Brandenberger, *Universe reheating after inflation*, *Phys. Rev.* **D51** (1995) 5438–5455, [hep-ph/9407247].

[86] P. B. Greene, L. Kofman, A. D. Linde and A. A. Starobinsky, *Structure of resonance in preheating after inflation*, *Phys. Rev.* **D56** (1997) 6175–6192, [hep-ph/9705347].

[87] G. N. Felder, J. Garcia-Bellido, P. B. Greene, L. Kofman, A. D. Linde and I. Tkachev, *Dynamics of symmetry breaking and tachyonic preheating*, *Phys. Rev. Lett.* **87** (2001) 011601, [hep-ph/0012142].

[88] G. N. Felder, L. Kofman and A. D. Linde, *Tachyonic instability and dynamics of spontaneous symmetry breaking*, *Phys. Rev.* **D64** (2001) 123517, [hep-th/0106179].

[89] J. Garcia-Bellido, D. G. Figueroa and J. Rubio, *Preheating in the Standard Model with the Higgs-Inflaton coupled to gravity*, *Phys. Rev.* **D79** (2009) 063531, [0812.4624].

[90] F. Bezrukov, D. Gorbunov and M. Shaposhnikov, *On initial conditions for the Hot Big Bang*, *JCAP* **0906** (2009) 029, [0812.3622].

[91] J. Repond and J. Rubio, *Combined Preheating on the lattice with applications to Higgs inflation*, *JCAP* **1607** (2016) 043, [1604.08238].

[92] M. P. DeCross, D. I. Kaiser, A. Prabhu, C. Prescod-Weinstein and E. I. Sfakianakis, *Preheating after Multifield Inflation with Nonminimal Couplings, I: Covariant Formalism and Attractor Behavior*, *Phys. Rev.* **D97** (2018) 023526, [1510.08553].

[93] M. P. DeCross, D. I. Kaiser, A. Prabhu, C. Prescod-Weinstein and E. I. Sfakianakis, *Preheating after multifield inflation with nonminimal couplings, II: Resonance Structure*, *Phys. Rev.* **D97** (2018) 023527, [1610.08868].

[94] M. P. DeCross, D. I. Kaiser, A. Prabhu, C. Prescod-Weinstein and E. I. Sfakianakis, *Preheating after multifield inflation with nonminimal couplings, III: Dynamical spacetime results*, *Phys. Rev.* **D97** (2018) 023528, [1610.08916].

[95] Y. Ema, R. Jinno, K. Mukaida and K. Nakayama, *Violent Preheating in Inflation with Nonminimal Coupling*, *JCAP* **1702** (2017) 045, [1609.05209].

[96] E. I. Sfakianakis and J. van de Vis, *Preheating after Higgs Inflation: Self-Resonance and Gauge boson production*, *Phys. Rev.* **D99** (2019) 083519, [1810.01304].

[97] B. J. Carr and S. W. Hawking, *Black holes in the early Universe*, *Mon. Not. Roy. Astron. Soc.* **168** (1974) 399–415.

[98] B. J. Carr, *The Primordial black hole mass spectrum*, *Astrophys. J.* **201** (1975) 1–19.

[99] A. M. Green, A. R. Liddle, K. A. Malik and M. Sasaki, *A New calculation of the mass fraction of primordial black holes*, *Phys. Rev.* **D70** (2004) 041502, [astro-ph/0403181].

[100] S. Young, C. T. Byrnes and M. Sasaki, *Calculating the mass fraction of primordial black holes*, *JCAP* **1407** (2014) 045, [1405.7023].

[101] J. C. Niemeyer and K. Jedamzik, *Dynamics of primordial black hole formation*, *Phys. Rev.* **D59** (1999) 124013, [astro-ph/9901292].

[102] I. Musco, J. C. Miller and L. Rezzolla, *Computations of primordial black hole formation*, *Class. Quant. Grav.* **22** (2005) 1405–1424, [gr-qc/0412063].

[103] T. Harada, C.-M. Yoo and K. Kohri, *Threshold of primordial black hole formation*, *Phys. Rev.* **D88** (2013) 084051, [1309.4201].

[104] I. Musco and J. C. Miller, *Primordial black hole formation in the early universe: critical behaviour and self-similarity*, *Class. Quant. Grav.* **30** (2013) 145009, [1201.2379].

[105] H. Motohashi and W. Hu, *Primordial Black Holes and Slow-Roll Violation*, *Phys. Rev.* **D96** (2017) 063503, [1706.06784].

[106] K. Ando, K. Inomata and M. Kawasaki, *Primordial black holes and uncertainties in the choice of the window function*, *Phys. Rev.* **D97** (2018) 103528, [1802.06393].

[107] C.-M. Yoo, T. Harada, J. Garriga and K. Kohri, *Primordial black hole abundance from random Gaussian curvature perturbations and a local density threshold*, *PTEP* **2018** (2018) 123E01, [1805.03946].

[108] C. Germani and I. Musco, *Abundance of Primordial Black Holes Depends on the Shape of the Inflationary Power Spectrum*, *Phys. Rev. Lett.* **122** (2019) 141302, [1805.04087].

[109] G. Franciolini, A. Kehagias, S. Matarrese and A. Riotto, *Primordial Black Holes from Inflation and non-Gaussianity*, *JCAP* **1803** (2018) 016, [1801.09415].

[110] J. M. Ezquiaga and J. García-Bellido, *Quantum diffusion beyond slow-roll: implications for primordial black-hole production*, *JCAP* **1808** (2018) 018, [1805.06731].

[111] C. Pattison, V. Vennin, H. Assadullahi and D. Wands, *Quantum diffusion during inflation and primordial black holes*, *JCAP* **1710** (2017) 046, [1707.00537].

[112] M. Biagetti, G. Franciolini, A. Kehagias and A. Riotto, *Primordial Black Holes from Inflation and Quantum Diffusion*, *JCAP* **1807** (2018) 032, [1804.07124].

[113] C. Pattison, V. Vennin, H. Assadullahi and D. Wands, *The attractive behaviour of ultra-slow-roll inflation*, *JCAP* **1808** (2018) 048, [1806.09553].

[114] L. Pinol, S. Renaux-Petel and Y. Tada, *Inflationary stochastic anomalies*, *Class. Quant. Grav.* **36** (2019) 07LT01, [1806.10126].

[115] D. Cruces, C. Germani and T. Prokopec, *Failure of the stochastic approach to inflation beyond slow-roll*, *JCAP* **1903** (2019) 048, [1807.09057].

[116] G. F. Chapline, *Cosmological effects of primordial black holes*, *Nature* **253** (1975) 251–252.

[117] B. J. Carr, K. Kohri, Y. Sendouda and J. Yokoyama, *New cosmological constraints on primordial black holes*, *Phys. Rev.* **D81** (2010) 104019, [0912.5297].

[118] B. Carr, F. Kuhnel and M. Sandstad, *Primordial Black Holes as Dark Matter*, *Phys. Rev.* **D94** (2016) 083504, [1607.06077].

[119] B. Carr, M. Raidal, T. Tenkanen, V. Vaskonen and H. Veermäe, *Primordial black hole constraints for extended mass functions*, *Phys. Rev.* **D96** (2017) 023514, [1705.05567].

[120] P. Montero-Camacho, X. Fang, G. Vasquez, M. Silva and C. M. Hirata, *Revisiting constraints on asteroid-mass primordial black holes as dark matter candidates*, 1906.05950.

[121] K. Inomata, M. Kawasaki, K. Mukaida and T. T. Yanagida, *Double inflation as a single origin of primordial black holes for all dark matter and LIGO observations*, *Phys. Rev.* **D97** (2018) 043514, [1711.06129].

[122] A. Katz, J. Kopp, S. Sibiryakov and W. Xue, *Femtolensing by Dark Matter Revisited*, *JCAP* **1812** (2018) 005, [1807.11495].

[123] H. Niikura et al., *Microlensing constraints on primordial black holes with the Subaru/HSC Andromeda observation*, *Nat. Astron.* **3** (2019) 524–534, [1701.02151].

[124] EROS-2 collaboration, P. Tisserand et al., *Limits on the Macho Content of the Galactic Halo from the EROS-2 Survey of the Magellanic Clouds*, *Astron. Astrophys.* **469** (2007) 387–404, [astro-ph/0607207].

[125] Y. Ali-Haïmoud and M. Kamionkowski, *Cosmic microwave background limits on accreting primordial black holes*, *Phys. Rev.* **D95** (2017) 043534, [1612.05644].

[126] S. W. Hawking, *Particle Creation by Black Holes*, *Commun. Math. Phys.* **43** (1975) 199–220.

[127] S. Alexeyev, A. Barrau, G. Boudoul, O. Khovanskaya and M. Sazhin, *Black hole relics in string gravity: Last stages of Hawking evaporation*, *Class. Quant. Grav.* **19** (2002) 4431–4444, [gr-qc/0201069].

[128] P. Chen and R. J. Adler, *Black hole remnants and dark matter*, *Nucl. Phys. Proc. Suppl.* **124** (2003) 103–106, [gr-qc/0205106].

[129] K. Nozari and S. H. Mehdipour, *Gravitational uncertainty and black hole remnants*, *Mod. Phys. Lett.* **A20** (2005) 2937–2948, [0809.3144].

[130] J. H. MacGibbon, *Can Planck-mass relics of evaporating black holes close the universe?*, *Nature* **329** (1987) 308–309.

[131] J. D. Barrow, E. J. Copeland and A. R. Liddle, *The Cosmology of black hole relics*, *Phys. Rev.* **D46** (1992) 645–657.

[132] B. J. Carr, J. H. Gilbert and J. E. Lidsey, *Black hole relics and inflation: Limits on blue perturbation spectra*, *Phys. Rev.* **D50** (1994) 4853–4867, [astro-ph/9405027].

[133] A. M. Green and A. R. Liddle, *Constraints on the density perturbation spectrum from primordial black holes*, *Phys. Rev.* **D56** (1997) 6166–6174, [astro-ph/9704251].

[134] A. Barrau, D. Blais, G. Boudoul and D. Polarski, *Peculiar relics from primordial black holes in the inflationary paradigm*, *Annalen Phys.* **13** (2004) 115–123, [astro-ph/0303330].

[135] P. Chen, *Inflation induced Planck-size black hole remnants as dark matter*, *New Astron. Rev.* **49** (2005) 233–239, [astro-ph/0406514].

[136] P. Ivanov, P. Naselsky and I. Novikov, *Inflation and primordial black holes as dark matter*, *Phys. Rev.* **D50** (1994) 7173–7178.

[137] J. Garcia-Bellido, A. D. Linde and D. Wands, *Density perturbations and black hole formation in hybrid inflation*, *Phys. Rev.* **D54** (1996) 6040–6058, [astro-ph/9605094].

[138] J. Yokoyama, *Formation of MACHO primordial black holes in inflationary cosmology*, *Astron. Astrophys.* **318** (1997) 673, [astro-ph/9509027].

[139] P. Ivanov, *Nonlinear metric perturbations and production of primordial black holes*, *Phys. Rev.* **D57** (1998) 7145–7154, [astro-ph/9708224].

[140] D. Blais, C. Kiefer and D. Polarski, *Can primordial black holes be a significant part of dark matter?*, *Phys. Lett.* **B535** (2002) 11–16, [astro-ph/0203520].

[141] J. Garcia-Bellido and E. Ruiz Morales, *Primordial black holes from single field models of inflation*, *Phys. Dark Univ.* **18** (2017) 47–54, [1702.03901].

[142] J. M. Ezquiaga, J. Garcia-Bellido and E. Ruiz Morales, *Primordial Black Hole production in Critical Higgs Inflation*, *Phys. Lett.* **B776** (2018) 345–349, [1705.04861].

[143] K. Kannike, L. Marzola, M. Raidal and H. Veermäe, *Single Field Double Inflation and Primordial Black Holes*, *JCAP* **1709** (2017) 020, [1705.06225].

[144] C. Germani and T. Prokopec, *On primordial black holes from an inflection point*, *Phys. Dark Univ.* **18** (2017) 6–10, [1706.04226].

[145] Y. Gong and Y. Gong, *Primordial black holes and second order gravitational waves from ultra-slow-roll inflation*, *JCAP* **1807** (2018) 007, [1707.09578].

[146] G. Ballesteros and M. Taoso, *Primordial black hole dark matter from single field inflation*, *Phys. Rev.* **D97** (2018) 023501, [1709.05565].

[147] LIGO Scientific, Virgo collaboration, B. P. Abbott et al., *Observation of Gravitational Waves from a Binary Black Hole Merger*, *Phys. Rev. Lett.* **116** (2016) 061102, [1602.03837].

[148] S. Downes and B. Dutta, *Inflection Points and the Power Spectrum*, *Phys. Rev.* **D87** (2013) 083518, [1211.1707].

[149] V. Faraoni, *A New solution for inflation*, *Am. J. Phys.* **69** (2001) 372–376, [physics/0006030].

[150] W. H. Kinney, *Horizon crossing and inflation with large eta*, *Phys. Rev.* **D72** (2005) 023515, [gr-qc/0503017].

[151] J. Martin, H. Motohashi and T. Suyama, *Ultra Slow-Roll Inflation and the non-Gaussianity Consistency Relation*, *Phys. Rev.* **D87** (2013) 023514, [1211.0083].

[152] K. Dimopoulos, *Ultra slow-roll inflation demystified*, *Phys. Lett.* **B775** (2017) 262–265, [1707.05644].

[153] Planck collaboration, Y. Akrami et al., *Planck 2018 results. I. Overview and the cosmological legacy of Planck*, 1807.06205.

[154] BICEP2, Keck Array collaboration, P. A. R. Ade et al., *BICEP2 / Keck Array XI: Beam Characterization and Temperature-to-Polarization Leakage in the BK15 Dataset*, 1904.01640.

[155] Simons Observatory collaboration. https://simonsobservatory.org/.

[156] Simons Observatory collaboration, J. Aguirre et al., *The Simons Observatory: Science goals and forecasts*, *JCAP* **1902** (2019) 056, [1808.07445].

[157] Euclid collaboration. https://www.euclid-ec.org/.

[158] L. Amendola et al., *Cosmology and fundamental physics with the Euclid satellite*, *Living Rev. Rel.* **21** (2018) 2, [1606.00180].